

AALBORG UNIVERSITY

MASTER THESIS

Waveform evaluation for 5G Networks

Author:

Pablo FUENTES PAZOS

Supervisors:

Gilberto BERARDINELLI

Troels B. SØRENSEN

*A thesis submitted in fulfilment of the requirements
for the degree of Master in Wireless Communication Systems*

in the

Department of Electronic Systems

June 3, 2015

AALBORG UNIVERSITY

Abstract

Faculty Name

Department of Electronic Systems

Master in Wireless Communication Systems

Waveform evaluation for 5G Networks

by Pablo FUENTES PAZOS

The Thesis Abstract is written here (and usually kept to just this page). The page is kept centered vertically so can expand into the blank space above the title too. . .

Acknowledgements

In this lines I would like to thank the people who have supported me during this master period and specially in the realization of this thesis. First of all I would like to express my sincere gratitude to my supervisors Gilberto and Troels, who had provided me a great support during all the project process. In the same line, I feel really thankful to Dereje for being always at my disposal whenever I needed and helping me facing the problems with a positive spirit. Moreover, I want to thank Manuel for the period working together.

For different reasons I'm also grateful to my friends Lucas, Germán and Laura who made me feel like home in this city since the day I arrived. Finally, I would like to stated my love and gratitude to my family, who are always there.

Contents

Acknowledgements	v
Contents	vii
List of Figures	ix
List of Tables	xi
1 Introduction	1
1.1 Introduction	1
1.1.1 Historical Perspective	1
1.1.2 Towards 5G	4
1.2 Project Definition	6
1.3 Report Structure	7
2 Waveforms for 5G	9
2.1 Requirements for 5G waveform	9
2.2 OFDM	11
2.2.1 Modulation schemes	14
2.2.2 Summary	17
2.3 SC-FDM	18
2.3.1 Concept	18
2.3.2 Modulation schemes	19
2.4 Zero Tail DFT-s-OFDM	21
2.5 Summary	23
3 Simulation	25
3.1 Simulation Software: LabVIEW	25
3.2 OFDM	28
3.2.1 Transmitter	28
3.2.2 Receiver	31
3.3 SC-FDM	34
3.3.1 Transmitter	34
3.3.2 Receiver	35
3.4 Zero Tail DFT-s-OFDM	36
3.4.1 Transmitter	36
3.4.2 Receiver	38

3.5	Results	38
3.5.1	Simulation scenario	39
3.5.1.1	AWGN channel	39
3.5.1.2	Fading channel	40
3.5.1.3	PAPR	42
3.5.2	OFDM	43
3.5.3	SC-FDM	46
3.5.4	Zero Tail DFT-s-OFDM	48
3.5.5	General comparison	50
3.6	Summary	52
4	Real Link Implementation	53
4.1	Introduction to the hardware	54
4.1.1	USRP N200	54
4.1.2	LabVIEW controller	55
4.2	Signal Adaptation	56
4.2.1	Synchronization	57
4.2.2	Phase error reduction	58
4.3	Real Link Scenario	59
4.4	Results	62
4.5	Summary	66
5	Conclusions	69
5.1	Project Summary	69
5.2	Conclusions	70
5.3	Future lines of study	71
	Bibliography	73

List of Figures

1.1	Evolution of mobile communications. Source: www.ofcom.org.uk	3
1.2	Global mobile data traffic. Source: Nokia White paper: 5G	5
2.1	Orthogonal subcarriers	12
2.2	Multipath delay spread	13
2.3	OFDM scheme for the transmitter.	14
2.4	OFDM scheme for the receiver.	16
2.5	Comparison of OFDMA and SC-FDMA transmission [7]	18
2.6	SC-FDM scheme for the transmitter.	19
2.7	SC-FDMA scheme for the receiver.	20
2.8	Interference between networks with different delay spread	21
2.9	Frame structures over scenario in Figure 2.8	22
2.10	Scheme and time signal for ZT DFT-s-OFDM	23
3.1	LabVIEW design example	27
3.2	OFDM Transmitter block diagram with graphical description	30
3.3	OFDM Receiver block diagram with graphical description	32
3.4	SC-FDM Transmitter block diagram	35
3.5	SC-FDM Receiver block diagram	35
3.6	Zero Tail DFT-s-OFDM Transmitter scheme	37
3.7	Tail generation	37
3.8	Zero Tail DFT-s-OFDM Receiver scheme	38
3.9	Power spectrum for a Additive White Gaussian Noise (AWGN) channel	40
3.10	Frequency selective fading channel realization	42
3.11	PAPR Comparison	43
3.12	BER performance of OFDM over AWGN channel	44
3.13	BER performance of OFDM over the fading channel (Urban Model)	45
3.14	Comparison of codes performance	46
3.15	BER performance of SC-FDM over AWGN channel	47
3.16	BER performance of SC-FDM over fading channel (Urban Model)	47
3.17	BER performance of Zero Tail DFT-s-OFDM over AWGN channel	49
3.18	BER performance of Zero Tail DFT-s-OFDM over fading channel (Urban Model)	50
3.19	BER performance over AWGN channel	50
3.20	BLER performance over AWGN channel	51
3.21	BER performance over fading channel (Urban Model)	52
3.22	BLER performance over fading channel (Urban Model)	52

4.1	LabVIEW scheme for USRP transmission	55
4.2	LabVIEW scheme for USRP transmission	57
4.3	QPSK constellation received.	58
4.4	Scenario representation	60
4.5	Transmitter and receiver disposition	60
4.6	BER comparison for 4QAM	63
4.7	BER comparison for 16QAM	64
4.8	BLER comparison for 4QAM	64
4.9	BLER comparison for 16QAM	65
4.10	Spectrum comparison	66
4.11	Time representation of Zero-Tail signal	66

List of Tables

3.1	PDP of the used channel models	41
3.2	OFDM configuration parameters	43
3.3	Encoders configuration	45
3.4	OFDM configuration parameters	48
4.1	USRP N200/XCVR2450 specifications	54
4.2	USRP and link configuration	62

List of Acronyms

AWGN Additive White Gaussian Noise

BER Bit Error Rate

BLER Block Error Rate

CP Cyclic Prefix

DFT Discrete Fourier Transform

FDMA Frequency Division Multiple Access

FFT Fast Fourier Transform

IDFT Inverse Discrete Fourier Transform

IFFT Inverse Fast Fourier Transform

ISI InterSymbol Interference

LTE Long Term Evolution

OFDM Orthogonal Frequency Division Multiplexing

OOB Out Of Band

PAPR Peak to Average Power Ratio

PDP Power Delay Profile

QAM Quadrature Amplitude Modulation

SC-FDM Single Carrier Frequency Division Multiplexing

SDR Software Defined Radio

SNR Signal to Noise Ratio

TDMA Time Division Multiple Access

USRP Universal Software Radio Peripheral

VI Virtual Instrument

Chapter 1

Introduction

1.1 Introduction

In this chapter we will start with an overview on the evolution of mobile and wireless telecommunication technologies to understand the importance of anticipating and adapting networks to the market exigent demands. Secondly, a concise definition of the project goals is carried out. Finally, we introduce how the report is structured, with a brief summary of the purpose for each chapter.

1.1.1 Historical Perspective

Since their first commercial appearance at the early 80s, the cellular networks have evolved in a vertiginous race. This evolution is stimulated and urged by the continuous increase in the demand of the subscribers in terms of accessibility, quality and speed. Besides, these networks are being developed in a polymorphic way so the services offered to the users are increasing in terms of quantity and complexity.

At first instance the mobile networks were designed to cope only with voice traffic over analogue channels. Standards were created to establish a proper regulation frame so the companies and organizations could work in the same line and guarantee a compatibility between networks and terminals. Two of the basic concepts introduced in

this first generation were the structure of the network divided in cells and the capacity of transferring a call to a different station when the user was moving during the conversation (*handover*).

The appearance of the digital technologies provided the second generation of wireless mobile networks with strong advantages. In this line, it was the beginning of the digital radio signals and its standards can be divided in two main groups depending on the channel access method, TDMA-based (the most important is GSM) and CDMA-based. From a network perspective, the waveform transmitted for both options were a evolution in mobile communications. In the case of GSM, the first systems were using a Frequency Division Multiple Access (FDMA), splitting the bandwidth in several carrier frequencies. Moreover, the resources for each of these frequencies were shared using a Time Division Multiple Access (TDMA) technique, splitting the voice or data information in fragments and transmitting them over time slots. From the user perspective, the main difference with the 1st generation was that in addition to the voice traffic it was also possible to send data at a very low rate. The communications were digitally encrypted and the networks started offering innovative services such as short text messages (SMS).

In between the second and the launch of the third generation we find what it is commonly known as 2.5G. In this category are included GPRS and the subsequent EDGE technology, that can be considered an expansion of GSM. This intermediate step is justified by the demand of higher data rates, that at the same time made affordable the creation of other services such as the MMS (Multimedia Message Service).

The third generation of mobile telecommunications technology is based on the standards designed around the specifications of the IMT-2000, a group specifically created by the ITU for this purpose. 3G uses W-CDMA as its most widespread technology providing better spectral efficiency with a bigger range of services. Among the several new features that this generation incorporated it can be highlighted the Internet access and wideband services. These allow the development of real time multimedia environments that supports services like video-conference or electronic commerce. The 3G data traffic rate for the downlink varies between approximately 400 kbit/s of the first standards and more than 100 Mbits/s for the latest releases (HSPA+)[1] [2].

The latest age in mobile communication, that we use nowadays is the fourth generation technically called IMT Advanced. Similarly to the preceding generations, the ITU is the responsible of regulating and setting the requisites for terminals and equipment that work under this technology. At the beginning there were two systems commercially deployed, Long Term Evolution (LTE) and WiMAX. Despite the companies were offering these brand as 4G, their characteristics didn't fulfil the whole requirements arranged by the ITU-R for the fourth generation standards. For example, in terms of data speed, the early LTE release 8 established target peak data rate of 100 Mbit/s in the downlink for the 3rd category equipment which is not enough to comply with the 4th generation requirements demanded [3]. Based on that, they are often considered as Pre-4G or 3.9G.

To cope with this gap, standardized by the 3GPP group it showed up LTE Advanced, which is an enhancement of the former LTE. One of the lines explored for improving the performance relies in the ability to get the most out of advanced topology networks. The creation of the so called heterogenous networks (HetNets) with the combination of macrocells with picocells or femtocells can boost the benefits of LTE-Advanced systems.

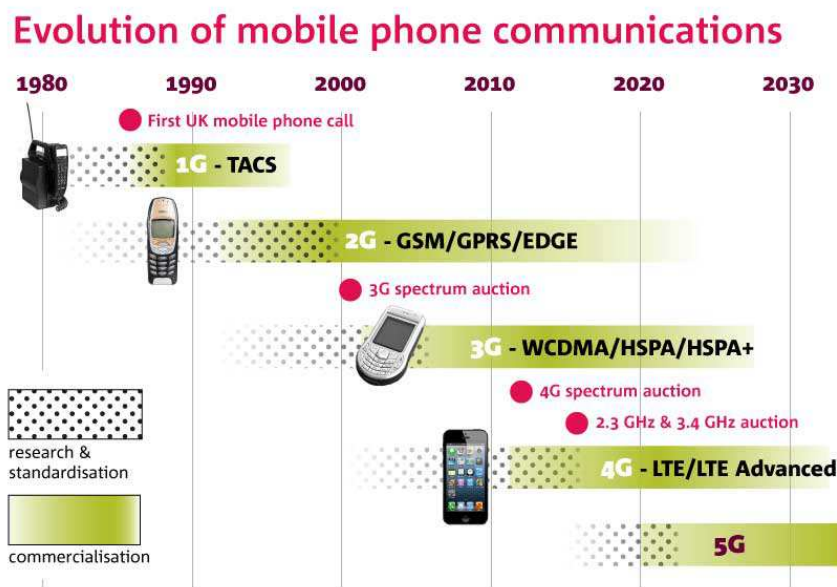


FIGURE 1.1: Evolution of mobile communications. Source: www.ofcom.org.uk

In Figure 1.1 it can be observed in a brief but concise way how the evolution of mobile communication has been since the early 80's. It is interesting how different generations coexist at the same time, what emphasise the importance of creating new

systems respecting the previous technologies. Besides, the data traffic rate needs special mention given its exponential increase over the years.

This growth is justified in some facts that affects to the new uses for this technologies. One of this reasons is the tendency to create and exploit services oriented or fully dependent on Internet access. Another fact is the development on media content quality, so the amount of data to be transmitted is every time bigger. In addition, the number of terminals demanding high speed access to Internet is also increasing [4].

Nonetheless, these new range of applications and services that are coming up not only push the limits for the data traffic rate. Some of them need the development on other characteristics, such as the latency, the reliability and security. One example of this, is the so called Tactile Internet, that makes mandatory a low delay in the response of the system.

1.1.2 Towards 5G

Currently we are in a phase characterized for the commercialization of 4G products. However, as it was discussed in the previous point, the market trend always points higher, so the investment and research on the future generation already started a few years ago. Almost every company and institutions in the sector is under the process of conceiving and studying different ideas to cope with the requisites foreseen for the fifth generation, expected to come around 2020. The predictions for the upcoming years are elaborated based in studies on long term historical tendency within information technologies, regarding several aspects, including the services already known to be incorporated in the near future.

One of these predictions can be seen in Figure 1.2. It represents the global data traffic expected for mobile communication from 2010 to 2030. It is based on an annual increase of the traffic volume per subscriber between 25% and 50%. Those predictions are represented by the two lines in the figure. As it can be seen, the progression grows exponentially, throwing an estimated global traffic for 2020 in a range from 100 to 1000 times higher than in 2010.

Regarding 5G, it is mandatory to size the upcoming generation to cope with a traffic for a longer period (e.g. 2030) so it guarantees a lasting lifetime. That brings

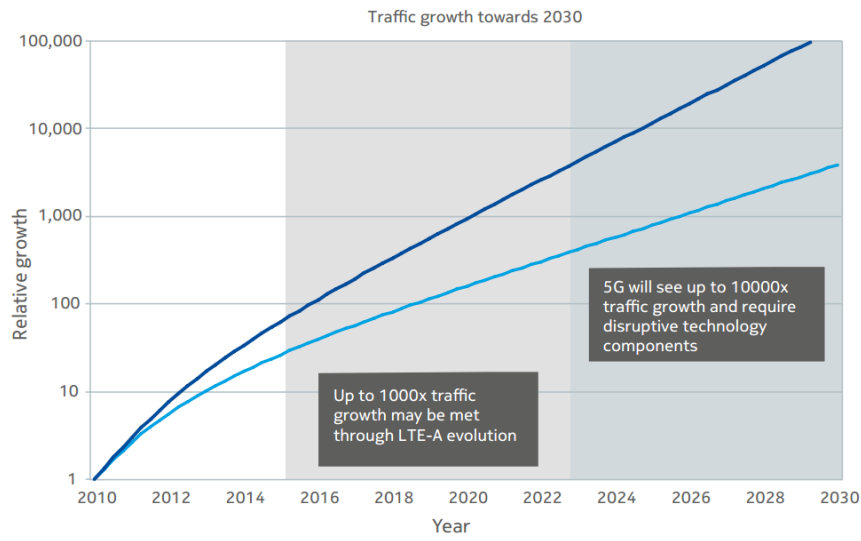


FIGURE 1.2: Global mobile data traffic. Source: Nokia White paper: 5G

an even wider gap to cope in the implementation and design of the new technologies. Such a great improvement can't be carried out only with small fixes to the present radio access technology, even more when existing 4G technologies present inner limitations to deal with those specifications. Thus, there are several aspects in the radio access design to reconsider, so the new generation has to be deeply redefined from its predecessor.

Two of these factors that will have an important role in 5G are the network cells deployment and the frequencies to be used. Concerning the first one, it is clear that future networks are headed to a structure of ultra-dense small cells. The number of picocells and femtocells are dependent on the density of subscribers in a certain area. Besides, it can be anticipated that incrementing the number of cells will be a very effective technique to improve the capacity.

Regarding the spectrum to be used there are two options considered, the centimeter-wave and the millimeter-wave. The millimeter-wave band is a spectrum range that has never been used before for this purpose, so the performance and propagation characteristics are partially unknown and have to be explored. Nonetheless, it is clear that higher frequencies imply relevant drawbacks, like hard link budget due to the propagation losses and the severe attenuation of potential obstacles. On the positive side, working at those frequencies offers a large spectrum to exploit and makes expendable some of the techniques used to increase the spectral efficiency. Moreover, to cope with

the severe link budget, the design of higher directional beam antennas based on large arrays can be carried out in smaller size, given the high operating frequencies.

On the other hand, the centimeter-wave band has similar characteristic to the spectrum used for 4G, so it represents a more familiar scenario. Conversely to the mm-wave concept, the line of sight condition for the communication link is not required. Nevertheless, the spectrum available at that range is not that wide, so it would still be significantly important to implement methods for efficient usage of the bandwidth.

As it can be noticed, so far we have just analysed 5G regarding the spectrum to be used and the presumable cell structure. However, 5G is still on the definition phase and there are several other characteristics and parameters with different options for their implementation that have to be decided. One of these characteristics conditioning the design of the radio access technique is the radio waveform.

The selection of the waveform type has a paramount impact in the complexity of the transceivers as well as in the link performance. Regarding the transceiver design it has to be remarked that some of the new services foreseen for 5G comprise the idea of a massive number of small devices, such as the so called concept of the Internet of Things (IoT). This leads to consider the simplicity and economy of the transceivers as a important factor. Moreover, the large number of subscribers also aims to new requirements like latency or energy efficiency. In addition to this, the Cognitive Radio (CR) idea of a flexible spectrum usage calls for the necessity of a well contained narrow-band signals with low out-of-band emissions.

As all these requirements are directly related with the radio waveform selection for 5G, it is clear the necessity of studying the advantages and disadvantages of the different options. In light of this, the present project is focused on the evaluation and analysis of the different waveform candidates from the perspective of coping with the upcoming generation requirements.

1.2 Project Definition

Within the 5G research, one of the questions that is still uncertain about the implementation of the Radio Access Technology is the radio waveform shape. Given

these circumstances, the main objective of this project is to carry out a study of the different options that can be implemented in the modulation. We consider and evaluate, among other waveform candidates, Zero-tail DFT-spread-OFDM. By this project we expect to determine the advantages and disadvantages of each model regarding to the complexity, performance and spectral containment. The project consist in two different phases:

- **Simulation phase.** In this stage we carry out the design and simulation of the waveform candidates using a software tool called LabVIEW from National Instruments. The models will be analyse from several perspectives (e.g. Bit Error Rate (BER), Peak to Average Power Ratio (PAPR)) in order to include most of the parameters with a relevant role in the decision of the radio waveform for the upcoming technology.
- **Implementation over real scenario.** The second phase consists in the implementation and testing of the candidates over a SDR platform based on USRP N200 by Ettus Research. Given the compatibility between this transceiver and the LabVIEW tool as a hardware controller, the schemes designed in the previous phase are fully portable for this purpose. The results of this test-bed proof will give a solid ground to the conclusions about the advantages and disadvantages of the waveforms evaluated.

1.3 Report Structure

For the sake of a clear understanding of the process followed for this thesis, it is kept a certain parallelism between the structure of the report and the different phases we went through for the elaboration of the project. The report is structured in 5 main chapters.

Chapter 1: Introduction The present chapter. A brief overview about the evolution of mobile communication and particularly in the upcoming fifth generation is carried out. Besides, it includes a project definition establishing the goals for the thesis.

Chapter 2: Waveform Models In this chapter we justify which types of radio waveform were chosen. Later, each modulation scheme is theoretically described to provide a solid background.

Chapter 3: Simulation The third section is centred in the simulation phase. First of all, we explain the main characteristics of the simulation tool. Afterwards, a description of each scheme implemented is carried out. Finally, we present the results obtained and we compare them with the theoretical results expected.

Chapter 4: Implementation This chapter is focused on the implementation of the link over a real scenario. In this section is included a description of the hardware used and the issues concerning the synchronisation between transmitter and receiver.

Chapter 5: Results On this section we will carry out a detailed exposition of the results gathered. Moreover, the outcomes for each waveform will be compared and discussed.

Chapter 6: Conclusions The last chapter is dedicated to the conclusions drawn over the whole elaboration process of the thesis.

Chapter 2

Waveforms for 5G

The present chapter will be dedicated to provide a theoretical overview of the waveforms evaluated on the project. To that end, we will firstly summarize the main properties expected for the 5G radio waveform in order to determine the most suitable line of research and its respective candidates. Later, a detailed explanation of the basis regarding the waveforms chosen will be conducted.

2.1 Requirements for 5G waveform

As it was presented in the introductory chapter, the objective of this project is to evaluate the possible waveforms that could be implemented for the 5th generation of radio access technology. The characteristics, structure and services that surround this new generation set a requirements frame to be suited by its waveform design. On this line, 5G is sketched to deal with peak data rates of 10 Gbps and operating with a latency under 1 ms [5]. To achieve this, the foreseen structure is expected to be formed by a massive distribution of small cells with limited coverage. The presumable interference caused by these deployment have to be compensated with techniques such as Interference Rejection Combining (IRC) or Inter-Cell Interference Coordination(ICIC) at the receiver. In addition, multiple-input-multiple-output (MIMO) antenna techniques are expected to play also an important role in the upcoming technology. Furthermore, novel types of communication will be supported by 5G, paying important attention to Device-to-Device (D2D) and Machine Type of Communication (MTC)[6].

Given this severe scenario and considering the determining influence that the radio waveform for 5G will have on the transceiver design and radio numerology, we could summarize the main properties of a suitable waveform candidate in these points [6]:

- Limited computational complexity. This would avoid the necessity of expensive equipment for generation and detection stages, which is particularly important for D2D and MTC communications oriented to presumable cheap devices.
- Limited time/frequency overhead. It is specially interesting if this overhead could be dynamically adapted regarding the link conditions.
- Good spectral containment. This would help in reducing or avoiding guard bands between systems operating over adjacent frequency bands.
- Good localization in time. It would significantly affect to the tracking process at the receiver, guaranteeing a low latency that will widen the potential services to offer.
- Robustness to hardware impairments. On this line, it is paramount a tolerance to the frequency offset and frequency drift characteristic of low cost devices.
- Easy adaptation to MIMO configuration without a high cost in computational complexity for the signal detection.
- Support for frequency selective link and rank adaptation. It is demanded a flexible adaptation to the frequency diversity of the radio channel. Thus, the modulation and the number of spatial streams can be set dynamically depending on the channel characteristics.

Reached this point, among the several options that are showing up in this process of selecting the waveform for 5G we could specially underline two candidates, Orthogonal Frequency Division Multiplexing (OFDM) and Filter Bank Multicarrier (FBMC) and Generalized Frequency Division Multiplexing (GFDM). All of them are multicarrier techniques, transmitting the data in parallel over multiple frequency subcarriers. The main difference between them is that OFDM uses a rectangular time-domain window for the pulse shaping while FBMC and GFDM implement more complex prototype filters in which frequency containment prevails. Because of this selectivity in frequency domain,

they have a better performance in Out-of-Band (OOB) emissions and are more robust to intersymbol interference. However, FBMC present some drawbacks like the high computational complexity needed for these prototype filters. Besides, a good symbol localization in frequency also carries a dispersive signal in time, that may lead to a significantly higher frame length non compatible with the low latency requirement. On the other hand, OFDM is a well-known technique given its presence in some technologies used nowadays, i.e. LTE (downlink). Among its several advantages we can underline the efficient use of the spectrum, the low complexity of the equipment needed and its efficiency from a computational perspective. It has also weak points such as a high Peak-to-Average Power Ratio (PAPR), excessive OOB emissions and a delicate sensitivity to frequency misalignment. Nonetheless, OFDM can be easily modified to overcome and reduce these limitations. For this reason we consider OFDM and the techniques based on it the strongest line of research for the 5G waveform choice.

In the following sections we will give a theoretical overview of the concepts involving Orthogonal Frequency Division Multiplexing (OFDM) and two other OFDM-based techniques that we consider suitable for the 5G requirements, DFT-s-OFDM and Zero Tail DFT-s-OFDM.

2.2 OFDM

Orthogonal Frequency Division Multiplexing (OFDM) is a modulation technique for the transmission of data over a group of subcarriers. The main benefit of this format is the orthogonality between the subcarriers, what brings the possibility of setting a very narrow space between subcarrier while avoiding their mutual interference.

Although OFDM is known for a long time, its practical application in wireless communication was unaffordable until recently, given the complexity of the equipment needed at both ends. However, OFDM practical implementation has become possible with the introduction of the IFFT. OFDM use is nowadays very extended, being the modulation technique implemented in LTE for the downlink. It is also the radio transmission format for the standards IEEE 802.11a/g (WiFi).

As it was previously said, the paramount feature of OFDM is the orthogonality between the subcarriers where the symbols are mapped. To explain this property we can start by examining the expression in time of a single subcarrier x_k in baseband:

$$x_k(t) = A_k e^{j\frac{2\pi kt}{T}} \quad 0 \leq t < T \quad (2.1)$$

In this equation the subindex k refers to the k -th subcarrier and T stands for the OFDM symbol period. The term A_k is the complex amplitude of the subcarrier, given by the symbol mapped at that frequency. For further considerations we will get rid of this amplitude since it does not affect to orthogonality. In order to check if two different subcarriers are orthogonal we calculate the cross-correlation over the period T :

$$R_{i,j}(t) = \frac{1}{T} \int_0^T x_i(t)x_j^*(t)dt = \frac{1}{T} \int_0^T e^{j\frac{2\pi t}{T}(i-j)}dt \quad (2.2)$$

From the expression 2.2 it can be concluded that the unique value for which the cross correlation will not be zero is for the condition $i = j$. Note that for this to be achieved we have considered a space between subcarriers inversely related with the symbol period ($\Delta f = 1/T$).

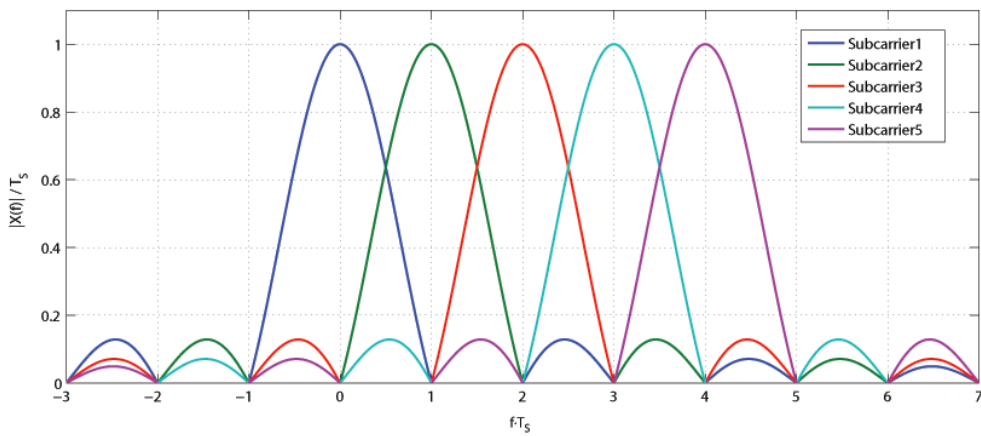


FIGURE 2.1: Orthogonal subcarriers

Figure 2.1 shows the spectrum in absolute value for the case of 5 subcarriers. As it can be observed, each subcarrier is located so its nulls coincide with the frequencies of the others subcarriers. Therefore, each channel can be demodulated at the receiver independently without any leakage from other subcarriers.

Cyclic Prefix

One important issue that has to be carefully considered when transmitting over environments characterized by multipath fading channels is the InterSymbol Interference (ISI). This phenomena shows up when the signal transmitted is spread and can take different paths, what directly result in a certain delay depending on the trajectory taken. This effect is represented in Figure 2.2

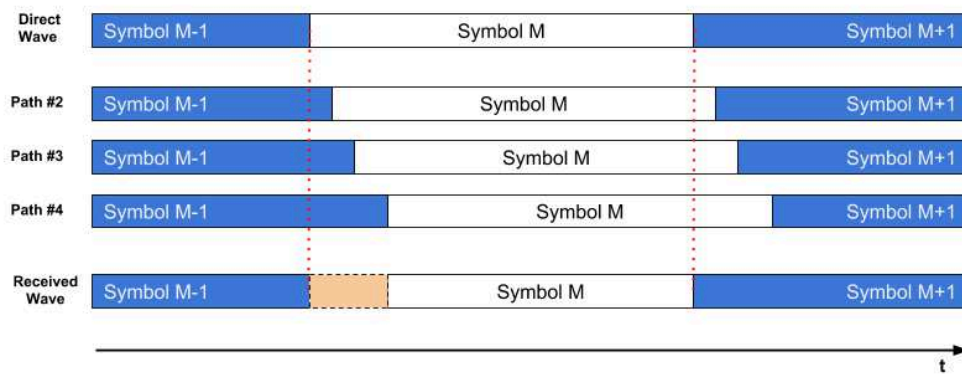


FIGURE 2.2: Multipath delay spread

The paths taken by non-direct waves arrive to the receiver with a certain delay, being the path #4 the one with the most delayed wave. As a result, there is an interval represented by the orange zone in which the symbol M from the direct wave is contaminated by the previous symbol transmitted through different paths. This time interval is called delay spread and is an important parameter when dealing with a specific radio scenario. Depending on the environment considered the delay spread can be significantly different.

The solution conceived for this intersymbol interference is the inclusion of a guard interval large enough to cover the delay spread. In the case of OFDM this guard interval is filled by copying the last part of the symbol and place it at the beginning. This portion inserted is called Cyclic Prefix (CP). One advantage of this method of filling the guard interval comes in the digital demodulation process. By this replica process

of transmitting the signal over the channel emulates a circular convolution between the former signal in time and the channel impulse response, resulting specially appropriate with the use of cyclic techniques for demodulation such as FFT.

2.2.1 Modulation schemes

One of the goals in this project is the simulation of the different modulation techniques that are candidates for the fifth generation of mobile communications. To set a proper background information, a review on the schemes used for the modulation and demodulation in these techniques will be given.

In the case of OFDM, the understanding of the blocks constituting the scheme is particularly relevant since many of the other access techniques can be considered as a modification of the one used for OFDM.

Transmitter

Figure 2.3 represents the basic scheme used for the transmission in a OFDM modulation technique. On it we can see the different blocks that take part in the modulation process.

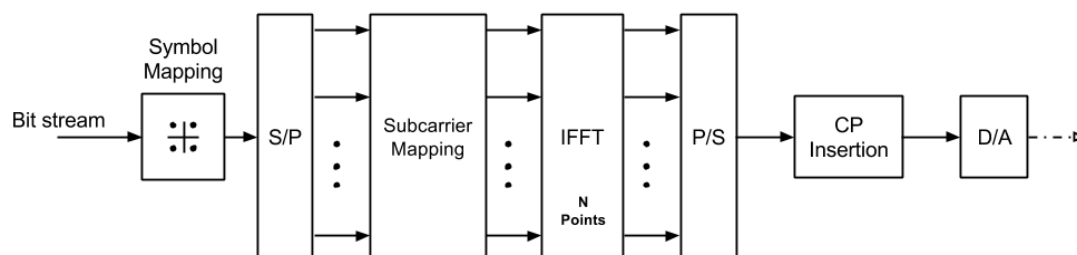


FIGURE 2.3: OFDM scheme for the transmitter.

Assuming a serial stream of binary digits as an input, the first procedure is the symbol mapping. The bits are mapped to a correspondent symbol stream using a modulation constellation. Dependent on the characteristic of the radio channel it can be selected a more packed constellation.

Next stage consist in the demultiplexing of the symbol stream into N parallel streams. N is determined by the number of subcarriers that are going to be used for the data transmission. In the subcarrier mapping block, the data is allocated along the subcarriers chosen for this purpose. In the case of OFDM the data subcarriers don't have to be all together, allowing free subcarrier between data. Generally only a portion of the subcarriers are used for the data and this factor can be set to combine various users over different subcarriers without any frequency collision. When the resources are shared among different users transmitting in the same time frame the technique is known as OFDM Access. Is important to make clear that each of these symbol streams are directly related with their correspondent subcarriers, so they will modulate the amplitude and phase of each of them.

Note that these two first blocks can be switched, dividing the bit stream into N separated streams and map each stream independently. This is the option used when wanting a different constellation depending on the subcarrier stream, suitable for frequency selective channels. Concerning the channel adaptation, the technologies using OFDM waveform signals dedicate one hard-coded OFDM symbol in each frame with a preset sequence to perform an estimation of the channel. These OFDM symbols are called Pilots and since they are not depending on the data and generated in a deterministic way, their values are known at the receiver.

The IFFT block corresponds to the Inverse Fast Fourier Transform and is the responsible of passing from frequency domain to time domain. This is a digital transformation and the size of the input (N_{IFFT}) determines the number of subcarriers that are considered. This number is typically a power of 2 to reduce the complexity of the operations and therefore the processing time. The inputs not used to transmit data are set to zero, leaving those frequencies empty. The main reason for this procedure is to keep a guard band between spectrums.

Once obtained the time taps from the IFFT, a parallel to serial stage follows to build the discrete signal in time. The signal obtained from each iteration of the IFFT is called OFDM symbol. Later, this signal is processed to insert the Cyclic Prefix which will be applied to each OFDM symbol. As it was said in the previous section, the length of the cyclic prefix is dependent on the radio channel characteristics and is a parameter that has to be agreed to use the same at both ends. The last block is the digital to analogue

conversion. This point reached, the sampling rate (IQ rate for complex signals) has to be calculated in function of the IFFT size (N_{IFFT}) and the desired subcarrier spacing (Δf_{sc}) following the equation 2.3. The resulting signal is allocated to the desired carrier frequency and transmitted to the channel.

$$IQ_{RATE} = \frac{1}{dt} = \Delta f_{sc} \cdot N_{IFFT} \quad (2.3)$$

Receiver

The scheme used for the OFDM receiver is represented in Figure 2.4. Most of the blocks used in the scheme are similar to the ones explained in the previous point, thus, just a brief exposition of their function will be state. As it can be observed in the figure, the distribution of the blocks is nearly symmetrical to the receiver, presenting at every step a block with an inverse functionality.

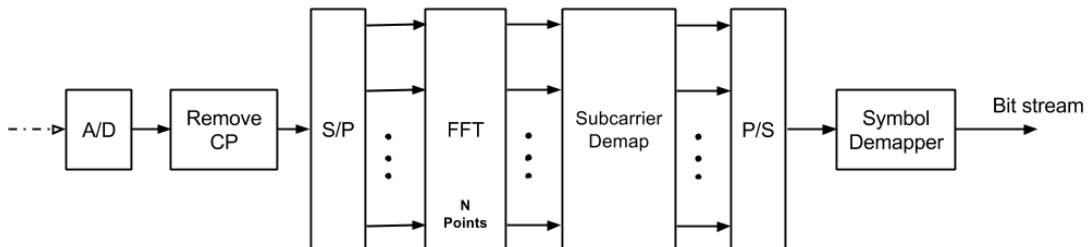


FIGURE 2.4: OFDM scheme for the receiver.

The first block is the analogue to digital converter, which will also work with a sampling frequency established in function of the number of subcarriers and the space between their respective frequencies. Once the signal is digitized, the next step is to remove the cyclic prefix. For this step is mandatory to have the signal synchronized at both frame and OFDM symbol level.

Before performing the FFT process, it is needed to take the taps from each OFDM symbol and pass them in parallel to the FFT block. Once the signal is again in the frequency domain, the symbols are extracted from the subcarriers. The pilots are separated

from the data and processed to estimate the channel. Since the pilots transmitted are known by the receiver, it can compare those values with the values received, establishing an equalization filter to reduce the effect of a frequency selective channel. There are different techniques to perform this equalization that will be considered and properly explained in the chapter regarding the schemes design.

Finally, the data symbols extracted are serialized to build the symbol stream and passed to the symbol demapper in order to get the bits demodulated at the receiver end.

2.2.2 Summary

To conclude with the exposition of the main theoretical concepts of OFDM we will resume its advantages and disadvantages. Among the strong points in the use of OFDM systems we can highlight the efficient use of the spectrum, taking benefit of the orthogonality between subcarriers. Another advantage is the way it divides the full channel in narrowband subchannels, keeping a good performance when dealing with frequency selective fading. This allows a simple equalization for each subchannel avoiding and isolating the detrimental effect of certain frequencies with a deep fading. One more benefit is the robustness against Intersymbol Interference (ISI) given by the insertion of the cyclic prefix. Finally, its implementation using FFT techniques turns OFDM into a very efficient method from a computational perspective.

On the other hand, OFDM also presents some drawbacks that can make it unsuitable in certain circumstances. The main weak point comes as the number of subcarriers increases, giving the signal in time a noise-like look with a high Peak to Average Power Ratio (PAPR) that requires linear transmitter circuitry, characterized by a poor power efficiency. This is the main reason why OFDM is not implemented in the uplink for LTE, given the necessity of power efficient terminals to prevent from battery drain.

Another disadvantage is that OFDM is very sensitive to frequency offset and drift. Any kind of frequency misalignment in the demodulation cause the loss of orthogonality between subcarriers. Furthermore, the natural solution to reduce the inefficiency of carrying the CP would be to set a larger OFDM symbol. This implies a consequent closer subcarrier spacing, that accentuates the harmful effect of frequency misalignment.

2.3 SC-FDM

The disadvantage of the high PAPR made OFDM unsuitable for the uplink given the power limitations regarding the mobile terminals. The Single Carrier Frequency Division Multiplexing (SC-FDM), also called DFT spread OFDM, appeared as a hybrid modulation scheme that combines some of the OFDM advantages with the low PAPR characteristic of a single carrier technique. The name DFT-s-OFDM is justified in the way the symbols are spread over the subcarriers using a DFT technique.

2.3.1 Concept

Although SC-FDM has strong similarities with OFDM in terms of implementation, the signal transmitted presents different properties. As it was introduced, SC-FDM came with the necessity of reducing the high crest factor inherent to multicarrier modulation techniques. To achieve that, the symbols are mapped in time and subsequently transform to the frequency domain. The rest of the process is analogous to the OFDM technique. For a clear understanding of the concept behind this procedure, we will rely on Figure 2.5.

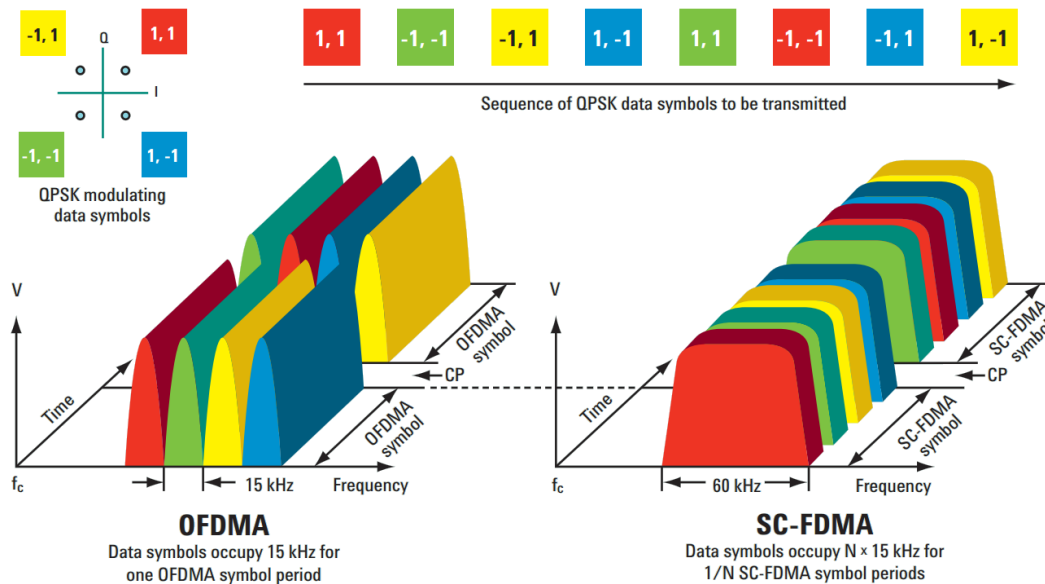


FIGURE 2.5: Comparison of OFDMA and SC-FDMA transmission [7]

Note that in this case, for a visual clarifying example we turn to OFDMA and SC-FDMA which are the multiple access versions for OFDM and SC-FDM respectively.

This difference is not important given that the waveform beneath the multiple access is the same. On the figure is shown a very simple example with four subcarriers and four symbols transmitted in parallel. Since the modulation considered is QPSK, all the symbols have the same amplitude and so the power of the subcarriers, leaning on the phase to distinguish them. The two plots for the signal transmitted with OFDMA and SC-FDMA have three axes each, meaning time, frequency and amplitude. The data symbol sequence has been coloured to contrast both cases.

For OFDMA, the QPSK data symbols are mapped directly to the subcarriers, transmitting them in parallel. The resulting OFDMA symbol is transmitted over a certain period, after which the cyclic prefix is added. To not mess with the graphical interpretation this was represented by a gap. Conversely, the SC-FDMA has a DFT pre-process of the data symbols, identifying a mapping over time. As a result, the data symbols are transmitted sequentially using the whole bandwidth. Thus, the SC-FDMA symbol period is the same as in OFDMA but distributed among the data symbols, concluding with a high individual rate. The main advantage of this technique is avoiding the parallel transmission of multiple symbols, which causes a high PAPR signal.

2.3.2 Modulation schemes

Basically the SC-FDM scheme is reached by adding a FFT stage previous to the IFFT block in the OFDM diagram. Since the scheme for OFDM was described in the previous section, the explanation here will be limited to the new block added and how it affects to the rest of the scheme. The structure for the transmitter is shown in Figure 2.6.

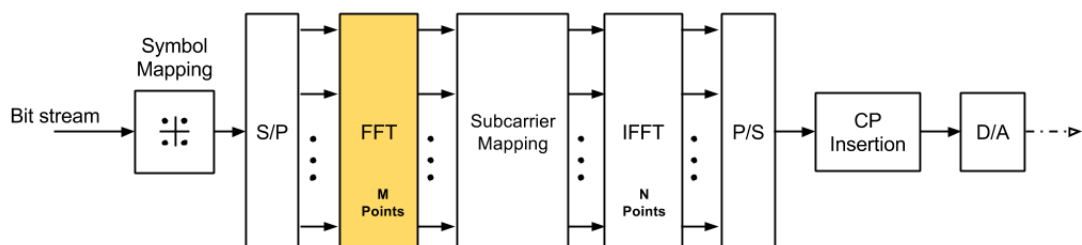


FIGURE 2.6: SC-FDM scheme for the transmitter.

It can be observed that the new block highlighted is placed between the serial to parallel phase and the subcarrier mapping. Note that the size of the FFT is different than the IFFT. This is justified by the fact that the IFFT operates over all the bandwidth subcarriers while the FFT make the transformation only for the group of subcarriers used for data transmission. This point reached, there are two strategies for mapping the M points of the FFT to the N subcarriers of the system. The first option is to map them over N adjacent subcarriers, what is called localized FDMA. The alternative is called interleaved FDMA and consists in distributing them over the M points of the IFFT, allowing free subcarriers between them. As explained in [8], the main drawback of this last strategy is that when various users have assigned a group of subcarriers, the spreading can cause some users to have more than 2 adjacent users, what enhances the harmful effect of a frequency offset.

Regarding the scheme for the receiver shown in Figure 2.7, the IFFT block of M points is symmetrically placed after the subcarrier demapping to take the signal back to time domain and extract the data symbols. In relation with this last DFT block it should be stated that the main drawback of SC-FDM is how this block spread the noise over all the subcarriers, with the consequent noise enhancement.

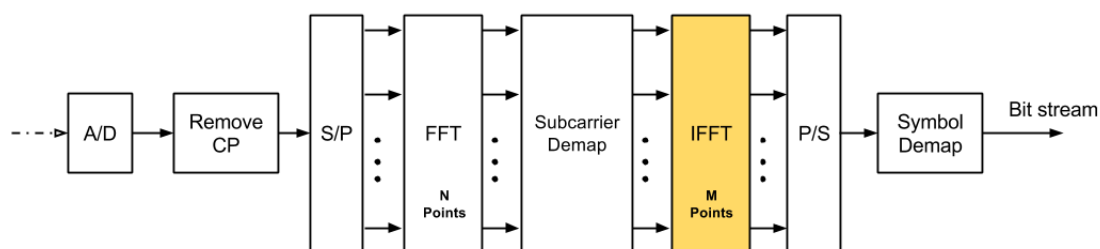


FIGURE 2.7: SC-FDMA scheme for the receiver.

2.4 Zero Tail DFT-s-OFDM

Motivation and concept

In section 2.2 it was explained why it was necessary the insertion of a guard interval to cope with the interference of adjacent symbols caused by multipath channels. In the case of OFDM and SC-FDM this guard interval was implemented as a cyclic prefix. In the existing technologies that use OFDM or SC-FDM, the length of this CP is a tradeoff between the estimated delay spread of the channel and the constraint of a predefined frame structure. For instance, in LTE there are two different options for the frame structure to deal with different channel characteristics, 14 symbols with a short CP of $4.7 \mu\text{s}$ or 12 symbols with a long CP of $8.3 \mu\text{s}$, fitting both cases the 1 ms subframe duration [9]. This limitation gives a poor flexibility for an accurate adaptation to the channel characteristics and may lead to a not efficient use of the resources when assigning a CP larger than the one needed or, on the other hand, the appearance of intersymbol interference if the CP doesn't cover completely a large delay spread.

However, another drawback for this strategy appears while dealing with networks operating in proximity over different frame structures, as depicted in Figure 2.8. Even when the frame structures are designed to be synchronized at frame level, the symbols have different lengths and would generate mutual asynchronous interference. This situation is graphically represented in Figure 2.9a

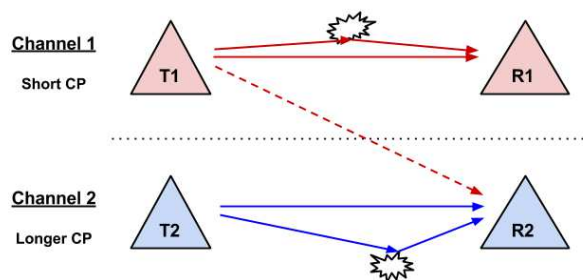


FIGURE 2.8: Interference between networks with different delay spread

Zero-tail DFT-s-OFDM is conceived as a modification of the DFT-s-OFDM to solve these problems regarding a hard-coded CP length. Instead of the CP insertion, the idea is to generate a tail of low power samples at the end of the symbols to cope with the delay spread of the channel. The length of this tail can be flexibly set to make an efficient

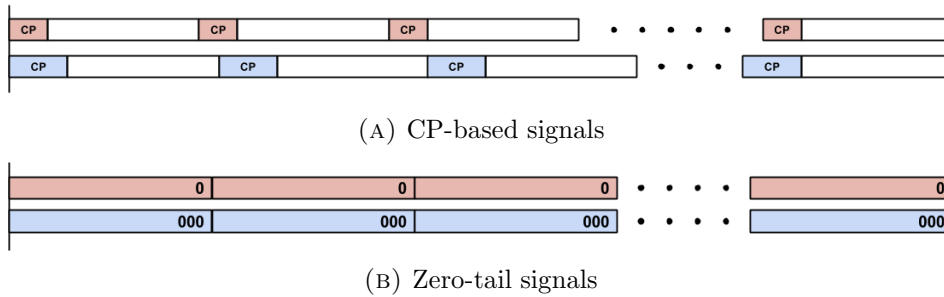


FIGURE 2.9: Frame structures over scenario in Figure 2.8

use of the channel, while respecting the symbol duration. In case the channel conditions are suitable the tail would be shorter, releasing resources for the pure data transmission. A comparison of the performance of Zero-tail and CP-based signals is carried out in Figure 2.9. The two main advantages of the Zero-tail signal are the granularity allowed in the length of the tail and the synchronization at symbol level. The first advantage consists in the flexibility in the selection of the length size, being able to closely adapt the tail to the delay spread of the channel. The synchronization at symbol level is particularly interesting, given that the mutual interference still present between networks operating with different tail size is synchronized and can be easily compensated with methods like Interference Rejection Combining (IRC) [10] and Successive Interference Cancellation (SIC) [11].

Tail generation

One consideration for ZT DFT-s-OFDM is that the zero tail is obtained as a natural output of the IFFT and not as a result of blanking the IFFT outputs. This allows the dynamic control of the tail from the symbol allocation phase, an earlier stage in comparison with CP-based technologies that insert the CP after the FFT process.

To achieve this, the Zero tail signals can be generated as a modification of the DFT-s-OFDM scheme. On this sense, the input of the FFT block will include a set of zeros at the end to origin a tail of low power taps after the DFT-IDFT process. It is also recommended the insertion of a small set of zeros at the beginning since the circular nature of the Discrete Fourier Transform provokes a power leakage from the first taps at the DFT input to the tail at the IDFT output. This header prevents from a power regrowth at the end of the resulting tail. A sketch of the scheme used for implementing

the Zero Tail DFT-s-OFDM is shown in Figure 2.10a. Moreover, an example of the resulting signal is plotted in Figure 2.10b.

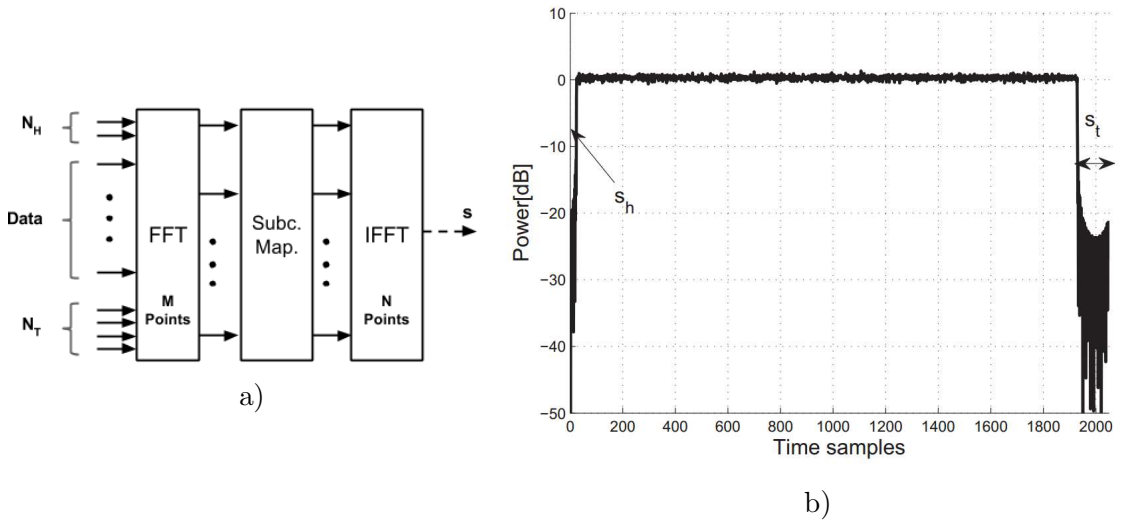


FIGURE 2.10: Scheme and time signal for ZT DFT-s-OFDM

The relation between the tail (or header) length of the resulting signal and the taps needed to be inserted is dependent on the size of the FFT and IFFT used in the implementation. It can be described as follows:

$$N_{S_{h,t}} = \left\lceil \frac{N_{h,t} N_{IFFT}}{N_{FFT}} \right\rceil \quad (2.4)$$

Thus, the transmitter has the possibility of adapting the tail to a certain delay spread, optimizing the resources dedicated for data transmission.

2.5 Summary

This chapter began with the exposition of the main properties that a radio waveform should accomplish in the frame of the new generation of wireless communications. Later, the three waveform candidates studied in this project were presented with a theoretical explanation. Moreover, it has also been explained their functional blocks as well as the main advantages and disadvantages for every candidate.

Chapter 3

Simulation

In this chapter we will address the transceiver design and link simulation of the waveforms candidates introduced previously. Firstly, an introduction to the software platform employed for the simulations will be carried out, paying attention to present the basic concepts of the tool that will help understand the designing process and limitations.

Secondly, the schemes for the transmitter and receiver of every waveform technique will be explained. After the transceiver design introduction, it will be described the channel scenarios implemented with the models used. In the last section we will present and discuss the results gathered, comparing them to the theoretical expected results in order to validate the schemes designed.

3.1 Simulation Software: LabVIEW

The first phase of the project consists in the simulation of the models that are considered suitable candidates for the upcoming 5th generation of wireless networks, that were theoretically introduced in the previous chapter. When carrying out a project involving the simulation of a system, is particularly important the decision about the software to be used. The characteristics that are considered more important when choosing a simulation software can be summarize in these points:

- The software should offer tools to implement and design a wide range of systems and techniques. This can be achieved by providing the user with a large number of functional blocks or functions.
- Simplicity of the programming language used. Many of the powerful software tools employed for simulations are based on complicated programming languages which make necessary a prior background to commit the task.
- Intuitive interface can make easier the debugging and error identification. In this line, the visual programming languages offer a clear interpretation of the system simulated and the blocks used on it, avoiding to dive in multiple lines of codes to identify and fix issues.

A simulation platform that acceptably achieve these properties is the LabVIEW software from National Instruments. However, the possibilities of this tool are not limited to a simulation environment, being also possible to use it as a hardware controller with the appropriate drivers. LabVIEW is a visual programming platform, which means that the design process is significantly more intuitive than other options operating under text-based languages. Besides, in addition to the huge database of functions that the basic version of LabVIEW includes, there are available online several extensions (called *toolkits*) with functions and blocks oriented to specific fields. One example of these *toolkits* is called Modulation Toolkit and provides useful integrated blocks for designing modulation and demodulation schemes. LabVIEW also provides the possibility of using scripts written in languages such as Matlab that are integrated in the scheme handling them as independent blocks.

Similar to LabVIEW there are other visual programming solutions like Keysight VEE developed by Agilent and the open source MyOpenLab. It is also worth mentioning other options like the one combining text-based languages Visual Basic, C++ and C# with a set of function libraries implemented by National Instruments and integrated in the Microsoft Visual Studio Environment.

Among all these candidates it was chosen LabVIEW for its flexibility and the availability of blocks and toolkits focused on radio waveform design. Moreover, is specially remarkable that LabVIEW is a tool highly compatible with the hardware used in the implementation phase of a real link. This fact makes possible a straightforward

adaptation of the scheme designed in the simulation phase to the scheme for controlling the hardware in the link implementation.

LabVIEW basic concepts

A program developed with LabVIEW is called Virtual Instrument (VI), given its appearance and working as a real instrument. In the same line, every VI has a part to interact with the user and a part equivalent to the source code where parameters from others VIs can be used. Analogously to a function in text-based languages, to interact with the user or higher instances some inputs variables are passed to the VI and the output variables are updated. The way the VI is implemented can be transparent to the user.

Concerning the design of a VI, there are two windows closely related with the two perspectives described previously: the block diagram and the front panel. The block diagram is the window where the raw design is carried out, inserting the blocks, variables and indicators used and how they are interconnected. On the other hand, the front panel is the graphical interface between the user and the VI. In the front panel the user can define the inputs to run the scheme and gather the output variables. A simple example of this LabVIEW interface is shown in Figure 3.1.

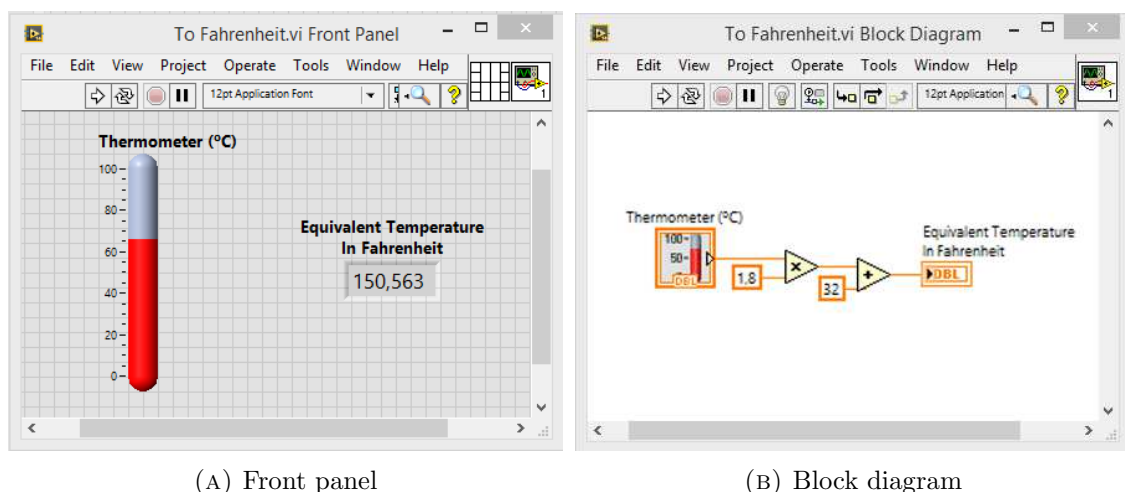


FIGURE 3.1: LabVIEW design example

One important feature of a VI is that it can be configured to be used as a subVI inside other schemes. This modularity of LabVIEW allows the user to create clear

and organized schemes, what consequently makes easier to identify designing errors or warnings that may affect to the VI operation.

3.2 OFDM

In the theoretical analysis of the waveform techniques realized in Chapter 2 it was shown the strong relation between the structures of the three models that are implemented. This reason given, the first technique implemented was OFDM to use it as a starting stage on which, with slight modifications in the structure, implement the two other waveform designs.

For the sake of a neat understanding the schemes designed will be depicted from a functional perspective, avoiding the explicit description of every VI used. Nonetheless, special attention will be paid to the configuration of every functional block as well as to the nature of the signals interconnecting them.

The design of the OFDM technique was carried out in different stages for verifying the scheme as more blocks were added until the complete link was implemented. Since in this software simulation stage the transmitter and the receiver are in the same design, the data simulated in the transmitter is also accessible in the receiver for the BER and BLER calculations.

3.2.1 Transmitter

The structure devised for the OFDM transmitter is shown in Figure 3.2. The functional modules forming the diagram are:

- **Bit generator.** For the binary stream that emulates the data flow feeding the system it was used a block that generates a float number with a uniform distribution. Later, this value is coerced and transform to a binary data type.
- **Encoder.** The design includes the possibility of encoding the binary data to get a better performance with error correction and detection. Since programming an encoder and the corresponding decoder from scratch is a laborious task, the type of encoders were limited to the ones available in the software Toolkits. Nonetheless,

it includes some interesting encoders like Convolutional, Hamming and BCH. The parameters for each type can also be set by the user from the front panel.

- **Interleaver.** This block is the responsible of shuffling the bits in a deterministic way to make the transmission more robust to a fading channel and enhance the forward error correction capability of the system. It was designed to reorder the bits within a window of 16 taps.
- **Symbol mapping.** After the binary stream is encoded and interleaved, the flow is mapped over the corresponding constellation. In this design, we rely on Quadrature Amplitude Modulation (QAM) techniques being able to choose in the front panel among 4-QAM, 16-QAM, 64-QAM types. By doing this, we keep a constant average power for the signal transmitted making easier the noise level set up.
- **Pilots insertion.** Once the signal is mapped over the QAM symbols, we proceed to insert the pilots for the channel estimation. The algorithm chosen for the pilots is a Zadoff-Chu sequence generator. Two useful properties that these sequences have is the constant complex amplitude and a very defined autocorrelation. The amplitude stability leads to a power efficient transmission as the signal has a low PAPR. The second property is specially interesting from the receiver point of view, being able to easily locate the pilots and consequently synchronise the frame faster. Besides, the system was designed to give the user a certain degree of freedom in the location of the pilots, being possible to select their position relative to the frame.
- **Subcarrier allocation.** As it was introduced in Chapter 2, OFDM usually uses just a portion of the spectrum available. Given this fact, the system was designed so the user can select the total number of subcarriers available (determined by the IFFT size) as well as the number of subcarriers dedicated to data transmission. In this line, the pilots use the same portion of bandwidth being transmitted by time domain multiplexing. For the OFDM simulation we will use one of the configuration used for the LTE downlink, using 300 data subcarriers out of 512[12]. Besides, the position of the empty subcarriers can also be defined, with the only restriction that all the data subcarriers have to be consecutively allocated.
- **IDFT.** This module transforms the vectors generated in the previous steps from frequency to time domain. LabVIEW implement this function with an Inverse

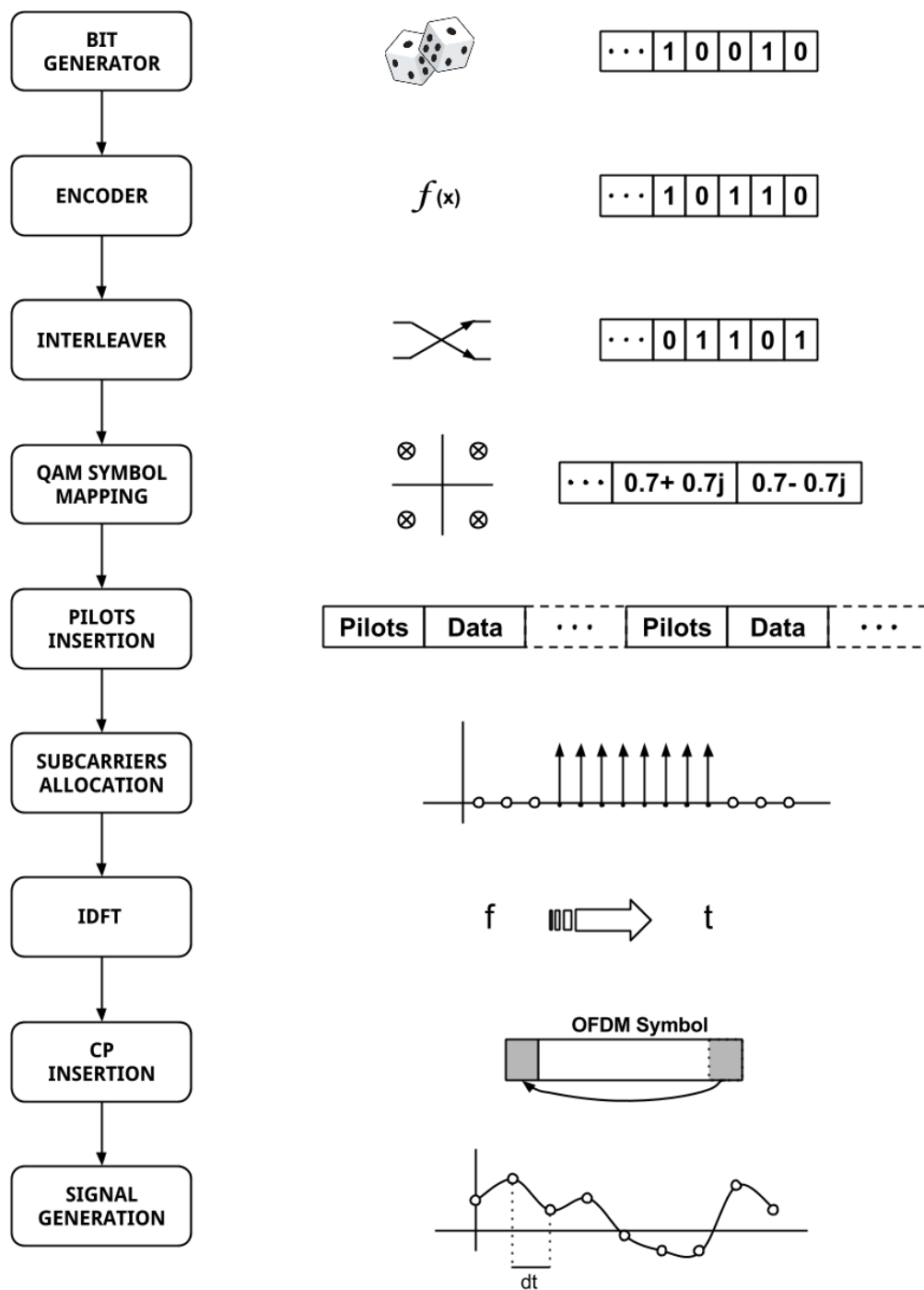


FIGURE 3.2: OFDM Transmitter block diagram with graphical description

Fast Fourier Transform (IFFT). Every OFDM symbol is considered as a vector, indexing each of them as rows in a matrix that represents the frame. The size of the IDFT transform is set to 512 in order to compute one vector at a time.

- **CP insertion.** When the signal is in time domain, the CP is added to the

beginning of each OFDM symbol. Although the CP in real practice is hard-coded, in our case the system allows to define a certain value as a percentage of the symbol duration to cope with ISI. After processing every vector from the array the outputs are concatenated so one large vector corresponding to the taps of the time signal is delivered to the next block.

- **Signal generation.** Finally, a waveform signal is built with the incoming vector and establishing a sampling rate (f_s). As it was aforementioned in Chapter 2 when the signal transmitted is complex, the sampling rate is referred as IQ rate and is related with the IDFT length and the subcarrier spacing in the following relation:

$$IQ_{RATE} = N_{IDFT} \cdot \Delta f_{sc} \quad (3.1)$$

3.2.2 Receiver

From the receiver point of view the structure is essentially the same with the inverse functionality of the ones forming the transmitter. The main difference is the necessity of estimating the channel response for a correct equalization of the signal received. Figure 3.3 shows the functional scheme for the OFDM receiver.

- Firstly the signal received is transformed from the digital waveform data type to a large vector with the amplitude of the taps, getting rid of the time reference. This can be done since the sampling rate is already known by the receiver.
- The vector containing the values of the temporal signal is reshaped as a matrix, placing each OFDM symbol in a different row and removing its CP.
- A DFT module processes the matrix and transform every symbol from time to frequency domain. In the same way as the IDFT, LabVIEW implements this function with a Fast Fourier Transform (FFT) block.
- The next stage is the subcarrier demapping, in which the receiver filters the empty subcarriers and select only the subcarriers used for transmission.

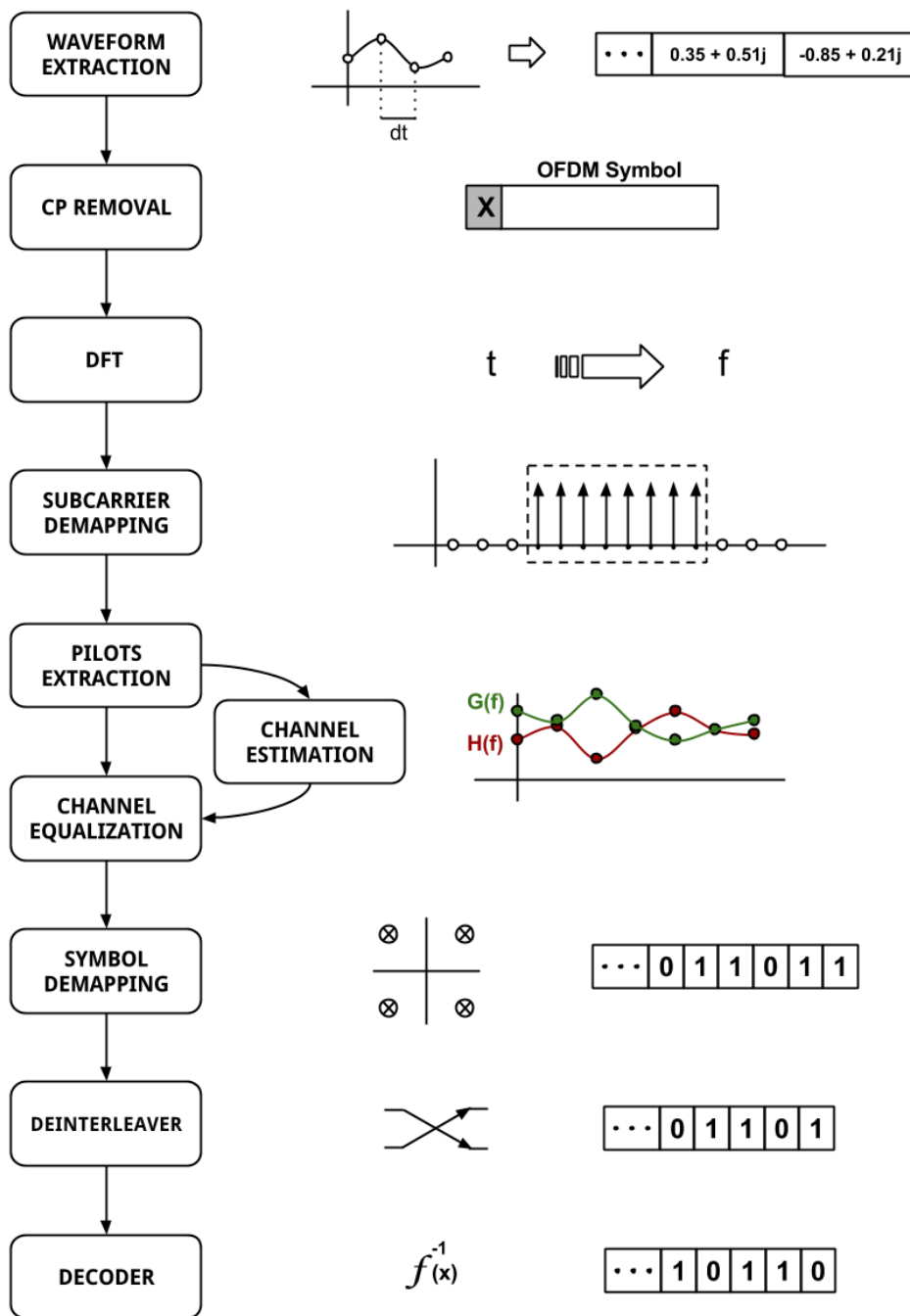


FIGURE 3.3: OFDM Receiver block diagram with graphical description

- At this point is when the main difference with the transmitter takes part. From the demapped subcarriers the receiver extract the pilots, which were generated in the transmitter with a deterministic function so they are also known at the receiver. The system compares the pilots received with the pilots that were transmitted to get an estimated channel response. Two methods were implemented to

reverse the distortion introduced by the channel, the Zero-Forcing equalizer and the MMSE equalizer. The Zero-Forcing equalizer is essentially applying the inverse of the estimated channel response. Equation 3.2 shows the mathematical expression for a Zero-Forcing equalization. The other option is the MMSE equalizer, which takes into consideration the noise level to minimize the mean square error between transmitted and received signal. The filter applied for this equalizer follows the equation 3.10[13].

$$C_{ZF}(f) = \frac{1}{\tilde{H}(f)} \quad (3.2)$$

$$C_{MMSE}(f) = \frac{\tilde{H}^*(f)}{|\tilde{H}(f)|^2 + \sigma_N^2} \quad (3.3)$$

Zero Forcing equalization counteracts perfectly the channel response removing all ISI. Nonetheless, when the channel is noisy, Zero Forcing will excessively amplify the noise in the frequencies where the channel response has a fading. In the case of OFDM this drawback is not particularly harmful since its multi-carrier nature constraint its effect just to the data sent in this range of frequencies making easy the error correction. On the other hand, in the single carrier techniques studied (SC-FDM and ZT DFT-s-OFDM) every data symbol is transmitted over all the subcarriers and consequently this noise boost would affect all the data transmitted, having a more detrimental consequence. As a result, single carrier techniques usually use MMSE equalization, characterized by its tradeoff between the ISI suppression and the control of the noise enhancement. For this to be achieved the equalizer needs an estimation of the noise level to compute the equalization filter.

- The QAM demapping process recovers the binary codified stream from the equalized data subcarriers.
- Finally, following the same procedure as the transmitter, the optional functionalities of binary deinterleaving and decoding are respectively carried out.

3.3 SC-FDM

Conversely to OFDM, Single Carrier Frequency Division Multiplexing (SC-FDM) is a single carrier waveform technique in which every symbol is transmitted over the whole bandwidth. However, from a designing perspective, both structures are closely related to the point that the SC-FDM transmitter can be implemented just by adding a DFT block prior to the subcarrier allocation. This small modification causes that symbols are no longer allocated in frequency but in time, and when the Fourier transform takes place they are spread over all the subcarriers.

The designing parallelism between OFDM and SC-FDM made possible the reuse of the schemes implemented on one for the other. Since a functional description of the blocks involved in the OFDM design was carried out in the previous section, at this point the explanation will be limited to the new blocks.

3.3.1 Transmitter

Figure 3.4 shows the additional stage that is included in the SC-FDM design. On it, it can be seen that the flow of symbols (S_K) generated in the QAM modulation stage build a complex sequence that can be considered as a discrete time signal. The DFT module is implemented with a FFT block available in the Modulation Toolkit. Its size is set to the number of subcarriers dedicated to data transmission, unlike the later Inverse Discrete Fourier Transform (IDFT) block that fits the whole bandwidth resources. For the SC-FDM simulation we will use the same bandwidth resources as in OFDM, setting the Discrete Fourier Transform (DFT) and IDFT sizes to 300 and 512 respectively. The mismatch between the DFT and IDFT used for the transmitter avoids a mutual cancellation effect so the QAM symbols are not directly mapped to the transmitted signal in time.

As it can be observed in the figure, the system was designed to insert the pilots after the DFT module. By this procedure, the channel estimation and equalization is made in frequency domain at the receiver, so those blocks remain the same as in OFDM.

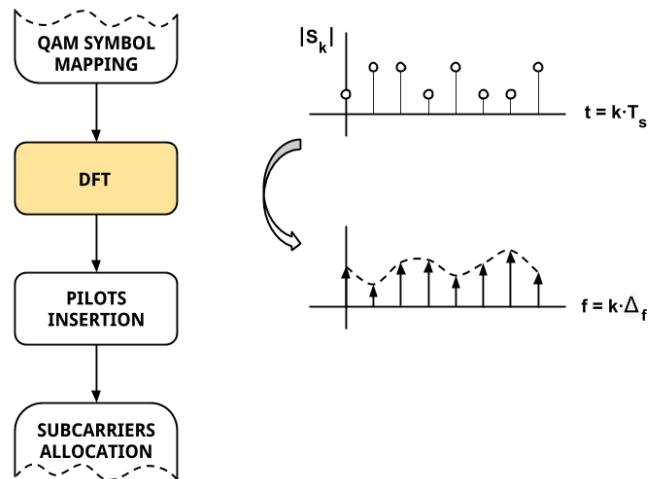


FIGURE 3.4: SC-FDM Transmitter block diagram

3.3.2 Receiver

The SC-FDM receiver takes the discrete signal in time and removes the cyclic prefix. This truncated vector is processed by the DFT stage to obtain the taps in frequency. Later, the channel estimation and equalization is made the same way as in OFDM. When the vector composed by the taps in frequency is equalized, the IDFT block transforms those taps to its time representation in order to extract the data symbols. This last procedure is shown in Figure 3.5.

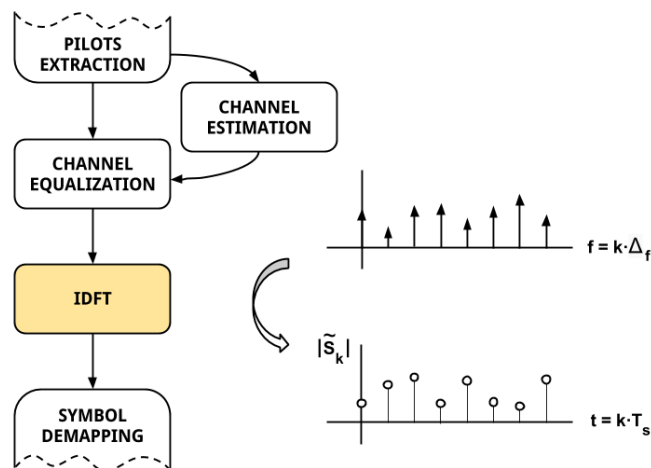


FIGURE 3.5: SC-FDM Receiver block diagram

Once the vector with the complex amplitude representing the data symbols is created, the next step is the QAM symbol demapping to make an estimation of the

binary chain that generated that sequence.

3.4 Zero Tail DFT-s-OFDM

Zero Tail DFT-s-OFDM was conceived with the idea of creating a waveform technique that could solve the intersymbol interference in a more efficient and advantageous way in comparison with the cyclic prefix. In the technologies implementing OFDM and SC-FDM, the length of the CP is hard-coded given the necessity of fitting a certain frame structure and timing. This lack of flexibility may end in a CP either too long or too short in comparison with the delay spread of the channel. When the CP is shorter than the delay there is a risk of having intersymbol interference, while on the other hand, if it is much larger, the system is wasting an interval of the CP that could have been employed for the transmission of useful data. The way Zero Tail DFT-s-OFDM accomplish this decoupling of the radio numerology and the expected channel characteristics is by generating the guard interval as a natural output of the IDFT block in the transmission.

3.4.1 Transmitter

Analysing the structure of a SC-FDM transmitter, it is easy to conclude that combining DFT and IDFT stages consecutively will establish a relation between the data symbols mapped to the DFT module and the signal transmitted after the IDFT process. Zero Tail DFT-s-OFDM uses this relation by adding a sequence of zero amplitude taps to the last positions of the DFT input in order to get a low power tail in the signal transmitted. The length of the sequence is directly related with the size of the low power tail and it can be set to cover the delay spread and suppress the ISI. As it was pointed in Chapter 2, a short head of zero symbols is needed to avoid the power regrowth at the end of the tail in the signal transmitted.

In summary, the resulting block structure for the Zero Tail DFT-s-OFDM transmitter is shown in Figure 3.6. The additional phase to insert the null sequences to generate the head and tail in the signal is coloured in orange. The rest of the scheme remains the same as in SC-FDM except for the CP insertion block, that was removed given that its functionality is substituted by the low power tail.

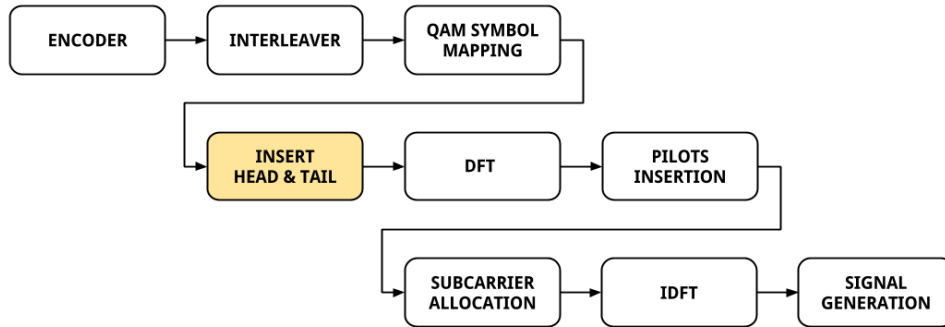


FIGURE 3.6: Zero Tail DFT-s-OFDM Transmitter scheme

The fact that both DFT and IDFT have different sizes causes the appearance of this low power tail signal instead of the null taps inserted to the DFT. This effect is depicted in Figure 3.7. Besides, it can be observed that the low power head contributes to smooth the transition between adjacent symbols in time, which may lead to a reduction of the Out Of Band (OOB) emissions.

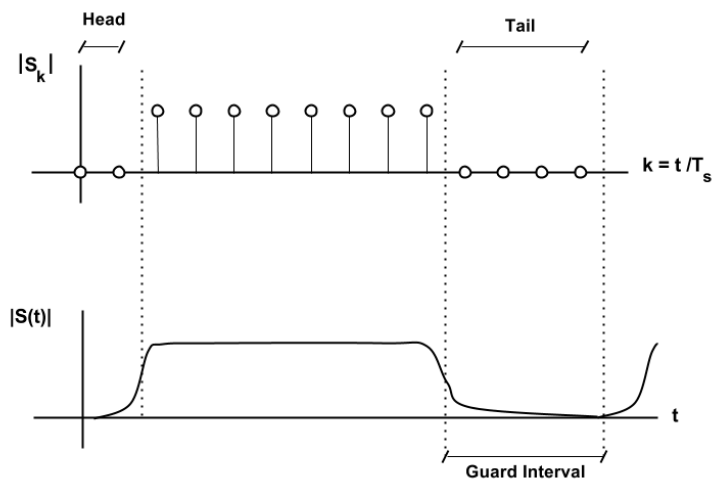


FIGURE 3.7: Tail generation

From the design point of view, the length of the tail should be adjusted to the expected channel delay spread and the head set to keep the tail power below a certain level. However, since the purpose of this project is to evaluate the performance of the different waveforms techniques for 5G, it is important to make a fair comparison between

the candidates, keeping a similar data rate in each waveform configuration. Since the length of the CP (OFDM, SC-FDM) and the head-tail (ZT DFT-s-OFDM) depends on the delay spread, they will be discussed in the section concerning the channel simulation.

3.4.2 Receiver

The design of the receiver follows the structure shown in Figure 3.8. The signal received is decomposed from the waveform data type into the dt parameter and the array containing the values of the signal in time. Every symbol is extracted from this array and transformed independently with the DFT. Once in frequency domain, the pilots are separated from the data to perform the channel estimation and the data is equalized and processed again with the IDFT block.

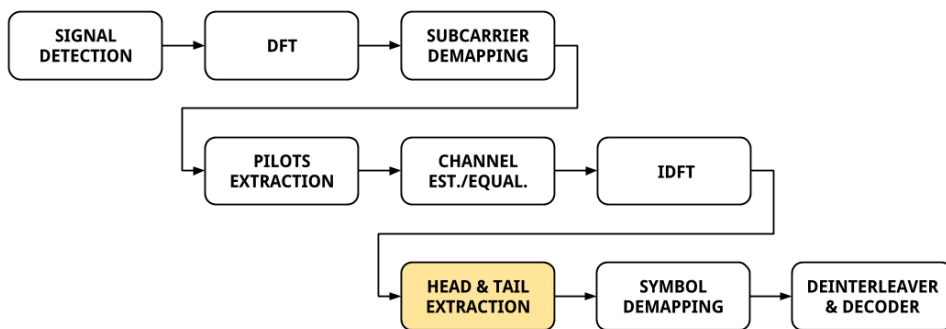


FIGURE 3.8: Zero Tail DFT-s-OFDM Receiver scheme

The next step is to remove the zero head and tail from the signal and demodulate the estimated QAM symbols received. After this stage the resulting bit stream is reordered and decoded.

3.5 Results

The main goal of this project is the evaluation of some of the most promising radio waveform candidates for 5G. In this chapter we have given a theoretical introduction of these candidates and presented the designing process of the schemes for the transmitters and receivers. This section will present and discuss the results obtained from the link

simulation of every candidate to study their performance regarding some relevant parameters involved in a radio waveform (e.g. BER, BLER or PAPR). Before presenting the results obtained, is necessary to introduce and explain the conditions considered for the simulation.

3.5.1 Simulation scenario

When carrying out a simulation of any system or technique is extremely important to properly configure the simulation parameters in order to suit and emulate the real working of the system as reliably as possible. In our case, there are many parameters that can be configured for each waveform technique simulated. Moreover, being the objective of this project the comparison between them, we have to pay special attention to the frame structures, establishing a fair comparison in terms of data throughput or bandwidth used. The transmitter and receiver parameters will be summarize in a table for every simulation carried out.

Besides the transmitter and receiver, it is particularly important the channel considered for the simulations. In the test followed we have implemented two channel models: Additive White Gaussian Noise (AWGN) and fading channel.

3.5.1.1 AWGN channel

The AWGN is a simple channel model that emulates the effect of many random processes that affect to the transmission. This model comprises the effect of these imperfections and represents them as a signal that will be added to the signal transmitted. From the frequency perspective the AWGN represents white noise, meaning a flat spectrum with constant spectrum density. Its behaviour in time is modelled by an additive noise signal with a complex Gaussian distribution. The standard deviation of this distribution is related with the spectrum density of the signal in frequency. An example of one AWGN channel realization is shown in Figure 3.9.

AWGN is a very basic model that doesn't take into account the effect of phenomenon like fading, frequency selectivity or dispersion, making it a not suitable model

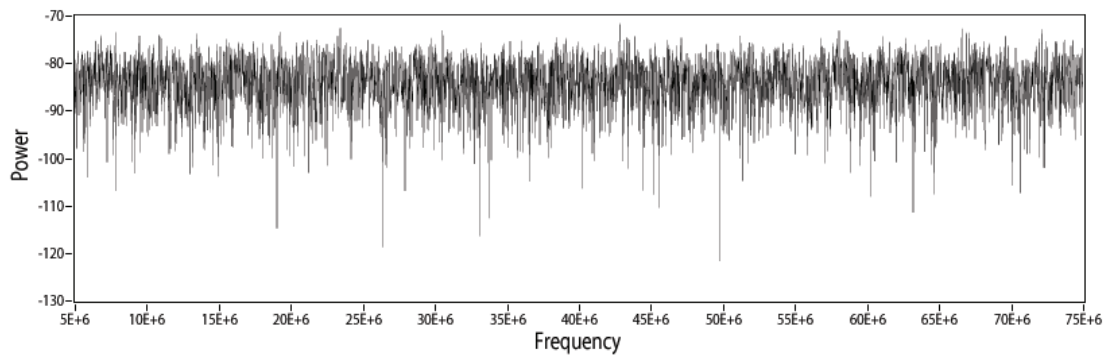


FIGURE 3.9: Power spectrum for a AWGN channel

by its own for communications in which these factors play an important role. However, is a very useful model in combination with models that mimic these other channel effects.

When analysing the performance of radio techniques it is common to express some factors in relation with the Signal to Noise Ratio (SNR) level. The SNR is the relation between the power of the signal transmitted and the average power of noise interfering, and acts as an indicator of how unfavourable are the channel conditions. In order to simplify the calculations, the average transmitted power will be normalized to 1. Thus, to simulate a certain SNR level it will be needed just to set the respective noise power of the AWGN channel. LabVIEW has available one block for the generation of a AWGN waveform, in which there are two parameters to define, the standard deviation of the noise and the sampling frequency. This block was modified to build a complex signal in time that would be later added to the transmitted signal.

3.5.1.2 Fading channel

One of the issues concerning the wireless communications is the environmental effect over the transmission. The reflections on the obstacles located between the transmitter and receiver can provoke the appearance of more than one paths followed by the signal transmitted. As a result of the reflections and propagation delay of every path, the receiver will have to handle a signal that is the superposition of several misaligned components with variations in amplitude and phase. When this situation occurs the channel is called Fading Channel.

There are different types of fading channels regarding aspects like time-variance, frequency response or the distribution type. In this line, if the number of transmission

paths is high and there is no remarkable predominance of the line of sight path, the statistical characteristics of the channel can be model as a Rayleigh distribution. This is the typical assumption for a scenario characterized by a dense urban location. Moreover, the frequency response of the channel will depend on the relation between the signal bandwidth and the channel coherence bandwidth, i.e. the range of frequencies over which the channel response can be considered stable.

Typical Urban		Indoor	
Delay (ns)	Power (dB)	Delay (ns)	Power (dB)
0	-5,7	0	-2.2
217	-7,6	5	-6.6
512	-10,1	5	-2.1
514	-10,2	5	-5.8
517	-10,2	15	-3.3
674	-11,5	15	-4.7
882	-13,4	15	-4.1
1230	-16,3	20	-8.2
1287	-16,9	20	-3.0
1311	-17,1	25	-5.2
1349	-17,4	30	-7.0
1533	-19,0	35	-4.6
1535	-19,0	40	-6.8
1622	-19,8	45	-8.6
1818	-21,5	80	-10.0
1836	-21,6	85	-12.1
1884	-22,1	110	-12.4
1943	-22,6	115	-11.8
2048	-23,5	150	-20.4
2140	-24,3	175	-16.6

TABLE 3.1: PDP of the used channel models

For the purpose of this project the channel was modelled by considering a Rayleigh distribution over a certain Power Delay Profile (PDP). The PDP represent the power of a pulse received through a multi-path channel in terms of the time delay between path arrivals. To generate the channel impulse response we first create a random complex variable under Rayleigh distribution using a Gaussian variable for both real and imaginary part. Then, the variance of this variable is modulated following the PDP. The two PDP used for the channel simulation are shown in Table 3.1. Besides the urban model, we also include the profile for simulating an indoor environment since the expected implementation measurements will be carried out in an indoor scenario.

In order to give a more graphical description of the models used, the frequency response of one channel realization is depicted in Figure 3.10. In this case, the profile used is the urban model. As it can be seen, depending on the frequency the subcarriers are located, they can experience a deep fading or operate over a relatively stable and good response.

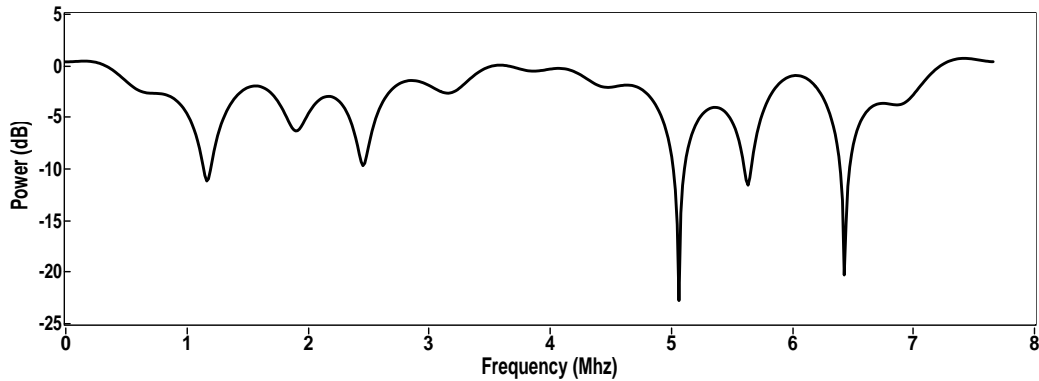


FIGURE 3.10: Frequency selective fading channel realization

3.5.1.3 PAPR

We will start by studying the PAPR performance for the three different waveforms since is an indicator of the signal profile and is not affected by the channel configuration. For this parameter we decide to include two configurations of the Zero-Tail technique to remark the influence of the tail and head size. The first one comprise a short tail of 10 taps with a header of a single tap. The second configuration is set for a 21 taps tail and a header of 2 taps. The PAPR was calculated applying equation 3.4 and getting one point per every OFDM symbol. In the formula $x(t)$ stands for the signal in time domain.

$$PAPR = \frac{\max[x(t) \cdot x^*(t)]}{\text{mean}[x(t) \cdot x^*(t)]} \quad (3.4)$$

The results, represented in Figure 3.11, present a high PAPR for OFDM, confirming its poor power efficiency. Moreover, comparing the curves between SC-FDM and

both Zero-Tail configurations, it can be concluded that the insertion of the low power tail reduces the average power of the signal transmitted and consequently increase the PAPR. It can be seen that for the case with a larger tail and header, the PAPR performance gets worse.

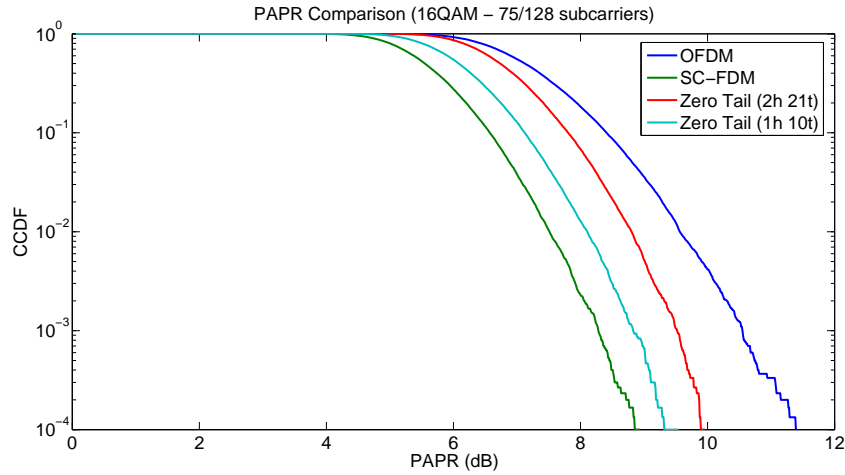


FIGURE 3.11: PAPR Comparison

3.5.2 OFDM

Once the PAPR performance was analyzed, now we will carry out the individual evaluation of the every radio waveform over the AWGN channel and the fading channel for the urban model. The first waveform technique designed and therefore simulated was OFDM, using it as the base model over which build the other schemes. The simulations will be focused in the analysis of the BER and the Block Error Rate (BLER).

IFFT size	512
No.subcarriers	300
OFDM Symbols/Frame	14
Subcarrier spacing	15 kHz
Position of the pilots symbol	1st symbol in frame
Equalization mode	Zero forcing
Cyclic prefix length	4.69 μ s
Modulations	4QAM, 16QAM, 64QAM

TABLE 3.2: OFDM configuration parameters

The configuration used for the OFDM simulation is described in Table 3.2. The values of the parameters were chosen in conformity with one of the formats for LTE. Thus, the structure consists in 300 subcarriers for data transmission with an IFFT size of 512. Each frame breaks down into 14 OFDM symbols, reserving the first one for the pilots transmission.

BER and BLER

In order to validate the scheme designed, it was necessary to compare some of the results obtained with the theoretical response expected. For this purpose it was used the MATLAB *bertool* program, which can generate the BER response in function of the E_b/N_0 for different QAM modulations over both AWGN and fading channel. Figure 3.12 shows the comparison between the theoretical and simulated results in the case of AWGN channel.

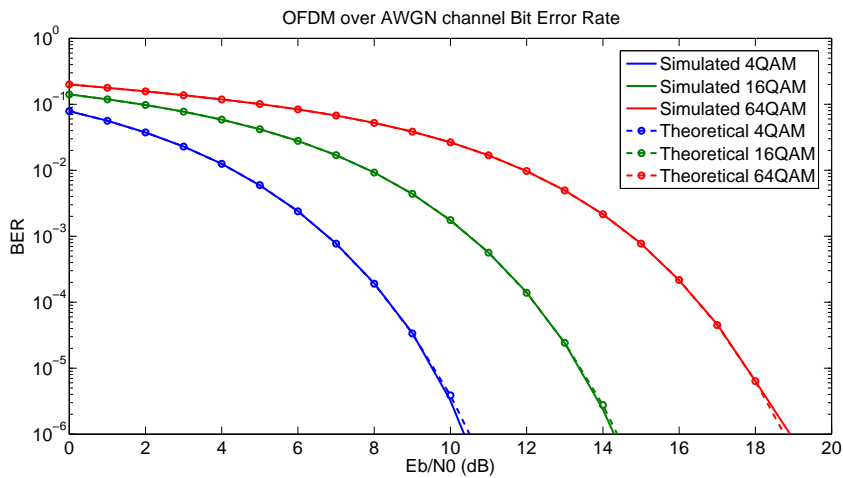


FIGURE 3.12: BER performance of OFDM over AWGN channel

As it can be seen, the results gathered from the simulations perfectly fit the expected curves for all the modulations considered. These matching results lead to a validation of the scheme implemented.

When the transmission is over a fading channel, the simulated results (Figure 3.13) also have the same response as the theoretical estimation. As it is guessed from the fading nature of the channel used, its BER curve is flatter than in the case of AWGN channel.

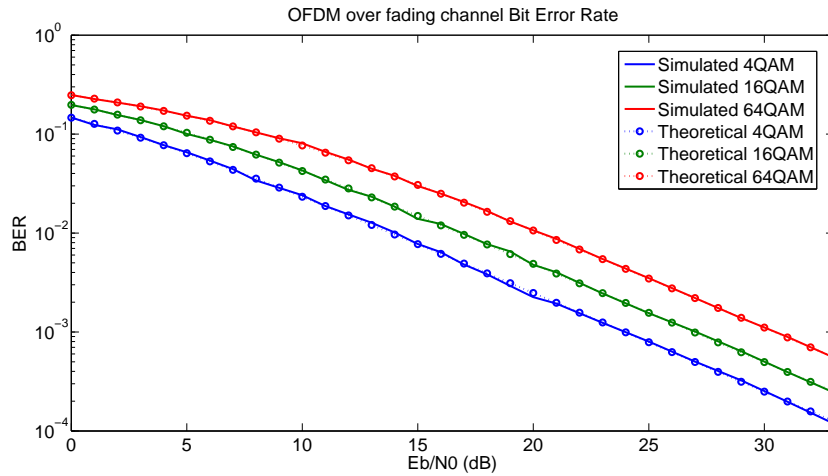


FIGURE 3.13: BER performance of OFDM over the fading channel (Urban Model)

Code Comparison

In addition to these results, as it was described in Chapter 2, the link simulated also include the option of adding an encoder and interleaver as a pre-process of the binary input stream. To that end, LabVIEW includes different types of encoders like convolutional, BCH or Hamming. The three of them are linear encoders, with the main difference that BCH and Hamming are block codes, while the convolutional encoder has a memory and generates the redundancy bits in function not only of the present values of the stream but with previous values as well. In order to make a quick study of the blocks offered, it was carried out a simulation of a OFDM link to compare their performance in terms of BER and BLER. The modulation used for this simulation is 16QAM and the configuration of each encoder is summarize in table 3.3. The parameters were selected in a compromise between efficiency and processing time.

Convolutional Encoder	Rate = 1/2 Constraint length = 7 Traceback depth = 35
BCH	Codeword length = 63 Length of message = 36 Correction capability = 5
Hamming	Order = 6

TABLE 3.3: Encoders configuration

The results of the simulations are shown in Figure 3.14, and it can be concluded that even when all the encoders manage to reduce the BER for high E_b/N_0 in comparison with the absence of encoder, they present a slight degradation in noisier conditions (below 6dB). This is caused by the fact that when the bit error probability is high, the redundancy trends to spread the errors to the correct bits. Nonetheless, the encoder with a better performance and therefore the one considered for the rest of the chapter is the convolutional encoder.

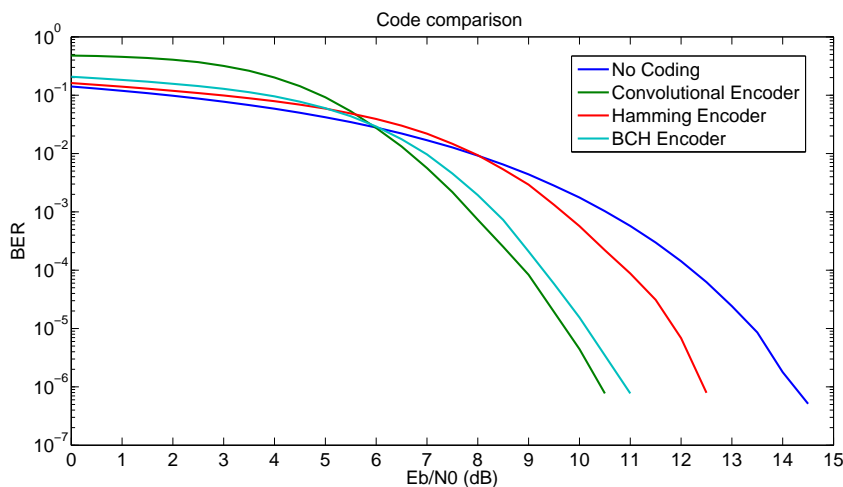


FIGURE 3.14: Comparison of codes performance

3.5.3 SC-FDM

For SC-FDM simulations the frame structure was preserved, with the DFT modification in the signal generation. The DFT size was adjusted to the subcarriers used in the transmission. In addition, the equalizer employed when considering a fading channel was also changed. The zero forcing equalization is substituted by the MMSE equalizer, more appropriate for a single carrier technique. The configuration set for the SC-FDM is basically the same as the one used for OFDM with the only difference of MMSE equalizer and the FFT size of 300 in the transmitter.

Since the basic OFDM and channel designs have been validated in the previous section, we will get rid of the theoretical approach from now on. In its place the performance for the case in which the encoder is present will be depicted.

BER and BLER

Figure 3.15 and Figure 3.16 represents the BER for the AWGN and fading channel respectively. In the case of AWGN channel the response is similar to OFDM given that the channel response in frequency is flat and the effect over the data transmitted is the same. On the other hand, it can be observed from the plot 3.16 a different performance, with a flatter response caused by the detrimental effect of the frequency selectivity in fading channels.

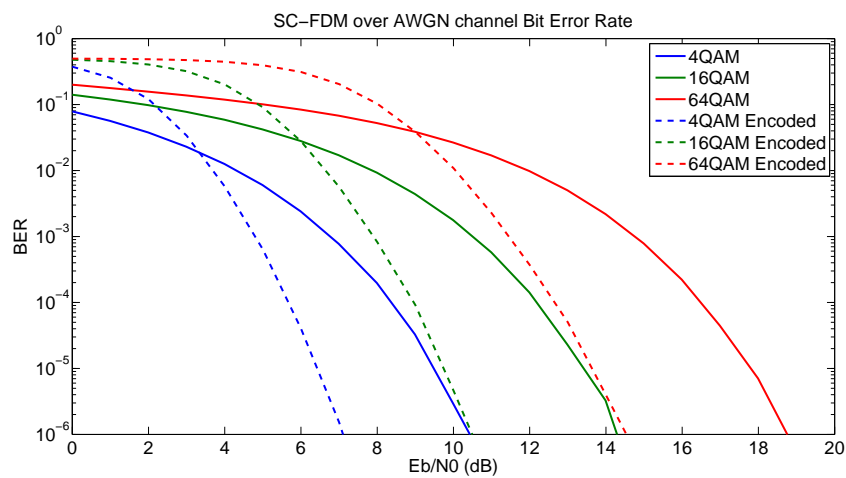


FIGURE 3.15: BER performance of SC-FDM over AWGN channel

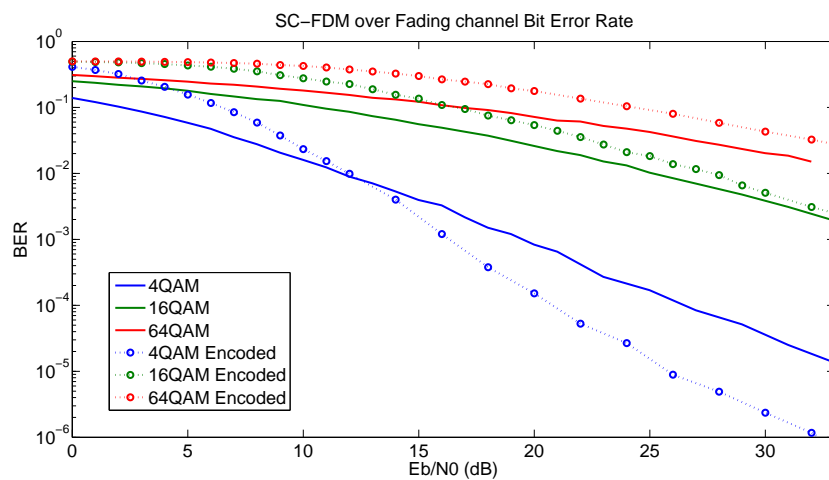


FIGURE 3.16: BER performance of SC-FDM over fading channel (Urban Model)

3.5.4 Zero Tail DFT-s-OFDM

The Zero-Tail DFT-s-OFDM technique differs from the SC-FDM in the generation and nature of the guard interval to cope with the ISI. These differences affect remarkably to the structure of the signal generated. To fairly compare this technique with the previous two waveforms it is necessary to design the system with a certain duration and structure of the frame so the data rate remains similar. To accomplish this, the configuration is set as shown in Table ??.

IFFT size	512
No.subcarriers	300
FFT size	300
Header and Tail taps	2+21 taps (preFFT)
OFDM Symbols/Frame	15
Subcarrier spacing	15 kHz
Position of the pilots symbol	1st symbol in frame
Equalization mode	MMSE
Tail length	4.66 μ s
Modulations	4QAM, 16QAM, 64QAM

TABLE 3.4: OFDM configuration parameters

The system reserve the last 21 taps of the DFT block for the tail generation while the header is limited to the first 2 taps. The frame consist in 15 symbols, being the first symbol dedicated for the pilots. The subcarrier spacing and the bandwidth used are not modified. Given this design, the comparison between the OFDM/SC-FDM structure and the one used for Zero-Tail stands like this:

OFDM/SC-FDM:

$$\frac{Symbols_{QAM}}{Frame} = 13 \cdot 300 = 3900 \quad (3.5)$$

$$T_{frame} = 14 \cdot \left(\frac{1}{15000} + 4.69\mu s \right) = 1ms \quad (3.6)$$

$$R = 3.9Mbauds \quad (3.7)$$

Zero-Tail DFT-s-OFDM:

$$\frac{\text{Symbols}_{QAM}}{\text{Frame}} = 14 \cdot (300 - 23) = 3878 \quad (3.8)$$

$$T_{\text{frame}} = 15 \cdot \frac{1}{15000} = 1ms \quad (3.9)$$

$$R = 3.88Mbauds \quad (3.10)$$

The similar throughput for both formats guarantee a coherent comparison.

BER and BLER

The BER response in terms of the SNR per bit is represented in Figure 3.17 and Figure 3.18 for the AWGN and fading channel respectively. Over a AWGN channel it gets more clear the key point in which the encoder overtake the non-coding curve. In the fading channel case, the performance is deteriorated being necessary a high E_b/N_0 to achieve an appropriate BER.

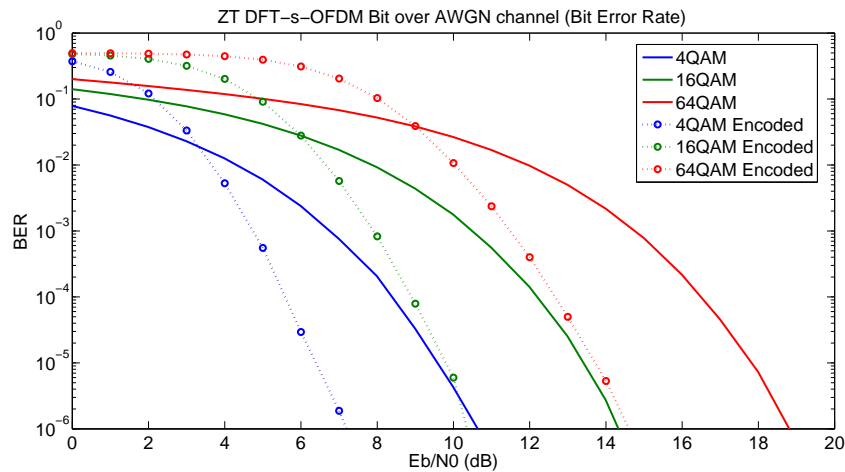


FIGURE 3.17: BER performance of Zero Tail DFT-s-OFDM over AWGN channel

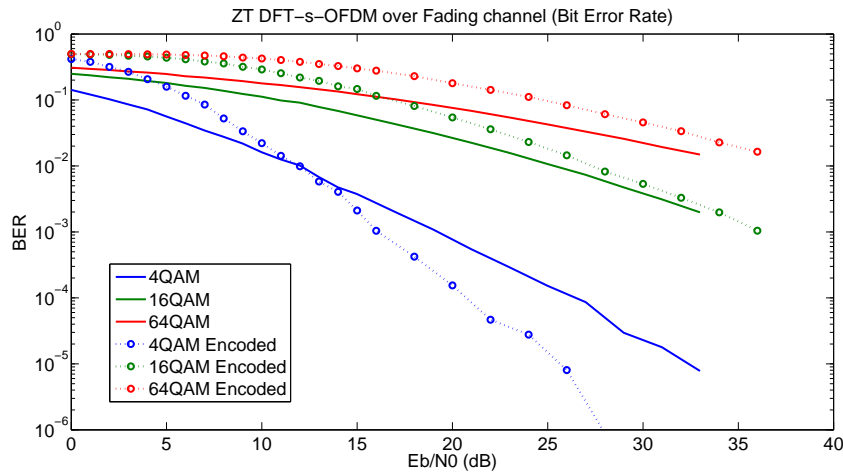


FIGURE 3.18: BER performance of Zero Tail DFT-s-OFDM over fading channel (Urban Model)

3.5.5 General comparison

Besides the analysis of each waveform by itself, the most interesting approach is comparing the results between the different techniques in order to get a reference of the relative performance, allowing to get some conclusions about the pros and cons of each candidate. For this purpose it will be plot in the same figures the performance of the different techniques. For the sake of not flooding the plots with curves, we will only consider the case of an uncoded transmission.

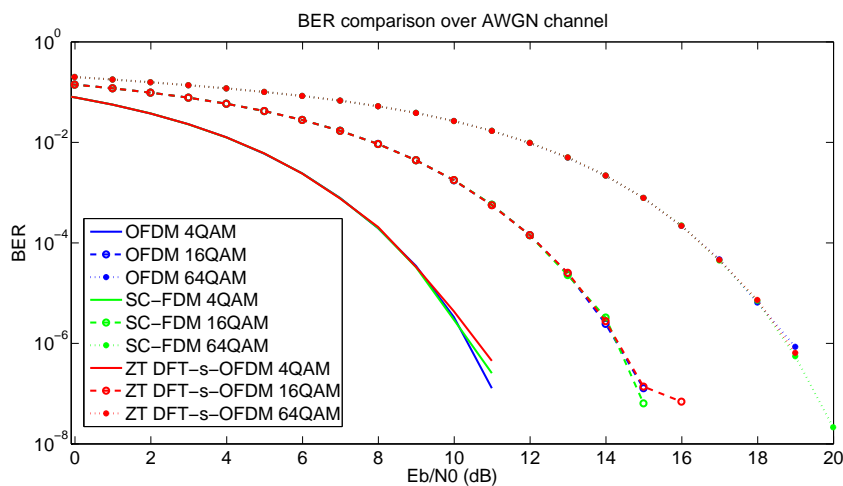


FIGURE 3.19: BER performance over AWGN channel

Figure 3.19 and Figure 3.20 show the BER and BLER respectively over an AWGN channel for the three techniques for the uncoded case. It can be seen that all the techniques have the same response in these cases. This is justified by the fact that the AWGN channel flat response in frequency affects statistically in the same way to one subcarrier than to the whole bandwidth. This makes no distinction between a multi-carrier technique (OFDM) and the single carrier waveforms (SC-FDM and ZT DFT-s-OFDM). However, when the channel introduces frequency selectivity the results

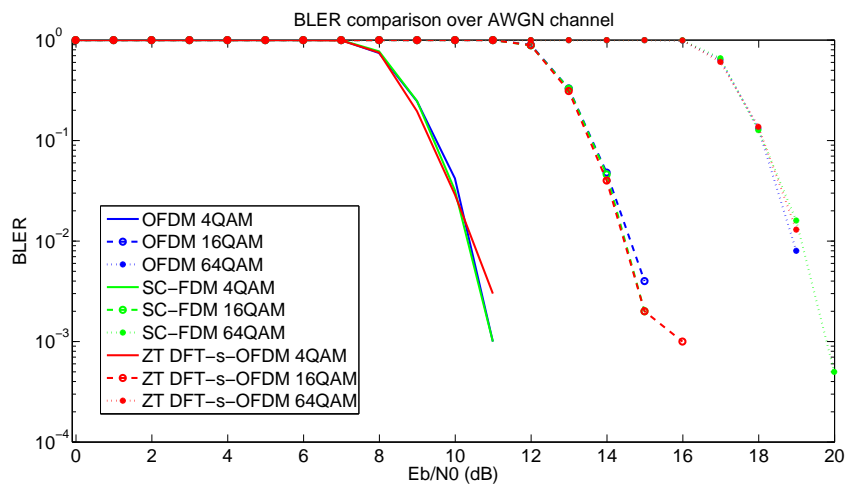


FIGURE 3.20: BLER performance over AWGN channel

of the techniques are different. This can be seen in the results over a fading channel for uncoded transmission, depicted in Figure 3.21 and Figure 3.22. These two plots show a close behaviour for both single carrier techniques regardless of the modulation employed, what makes sense given that the differences in the guard interval generation should not affect significantly to the BER or the BLER response. However, what is interesting from these plots is how affects the constellation to the BER and BLER performance. For 4QAM modulation, single carrier techniques present a better performance at high SNR in both BER and BLER plots. Conversely, for the cases of a more crowded constellation like 16QAM or 64QAM the BER and BLER of OFDM overcome the performance of SC-FDM and Zero-Tail. It can be seen that the higher the modulation the more deteriorated is the single carrier techniques performances.

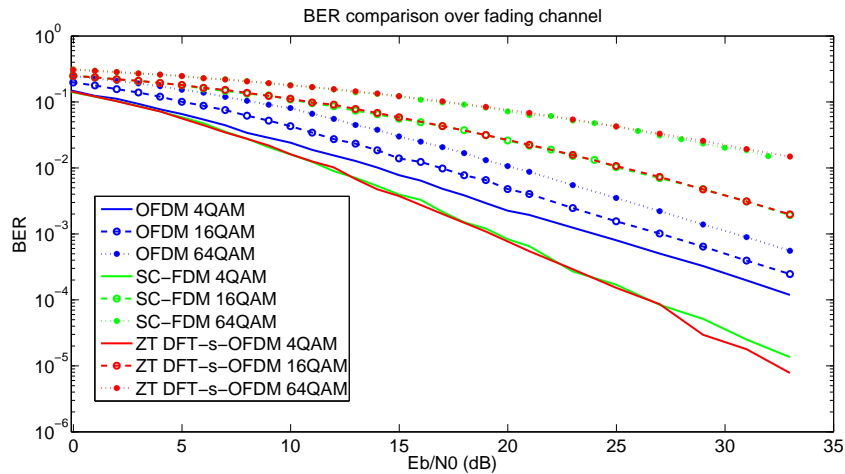


FIGURE 3.21: BER performance over fading channel (Urban Model)

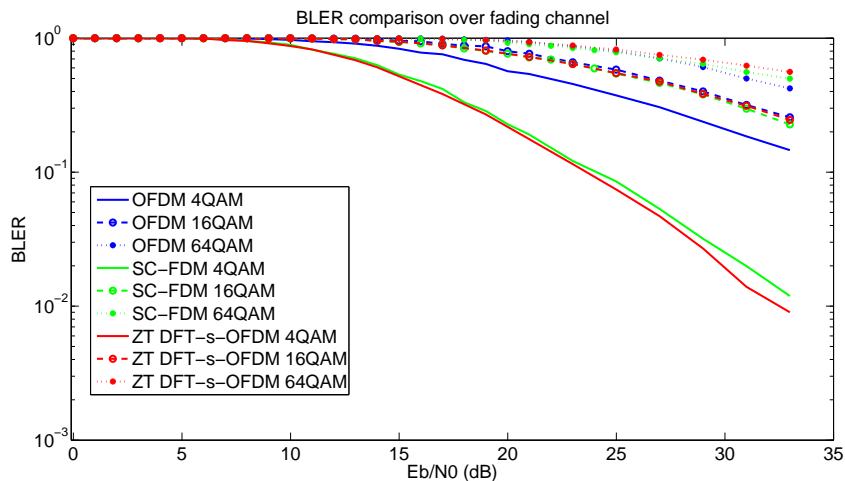


FIGURE 3.22: BLER performance over fading channel (Urban Model)

3.6 Summary

In this chapter we have addressed the simulation phase of the project. At first place we have introduced the software used for the simulations, including a brief explanation on how is the designing process for the LabVIEW platform. Later, we have analysed the radio waveforms from a functional perspective to have an idea of the structure followed during the schemes design for the simulations. Finally, the results collected were presented, contrasting some of them with the theoretically expected in order to validate the designs.

Chapter 4

Real Link Implementation

After a theoretical approach in Chapter 2 to the waveform techniques studied in this project, in Chapter 3 a link simulation was carried out using a software simulation tool. In this case, the entire link was simulated with LabVIEW, including different channel models. The results of these simulations are useful to provide an idea of how the system could perform under real circumstances. Nevertheless, the conclusions arose from these results have a limited reliability given the several factors affecting the real communications that are not taken into consideration or accurately emulated in a software simulation. For this reason, in order to properly evaluate the techniques studied in this project is determining to analyse the response over a real link.

The present chapter addresses the scenario setup for a real link testbed as well as the configuration of the elements involved in its realization. It will start by introducing the transceivers employed and the interface between them and the software toolkit. Later, we will describe from a topological point of view the scenario where the experimental results took place. Finally, a summary of the link configuration will be done. On this last point, special attention will be paid to explain the methods followed to synchronize the transceivers and reduce the phase noise present in the experiments.

4.1 Introduction to the hardware

The simulation of the link over a real scenario was carried out using the Ettus Research Universal Software Radio Peripheral (USRP) N200 transceivers. This hardware was previously used in the department to test other techniques and was proved to be a flexible tool for building SDR links. In this section, we will describe the main characteristics of the N200 series as well as how they are controlled using the LabVIEW tool.

4.1.1 USRP N200

The USRP N200 is a transceiver created by Ettus Research that was designed with the purpose of prototyping and building Software Defined Radio (SDR) systems in combination with a computer. USRP transceivers are a flexible and economic platform that provide researchers and students with the possibility of designing and testing RF systems in an easy and accessible way. In particular, the model N200 is compatible with GNU Radio, Simulink and LabVIEW. Since the simulation phase of the present project was also developed with the LabVIEW tool, this platform represents a straightforward opportunity to implement a real link relying on the schemes already designed.

The hardware used for the experimental phase is specifically a USRP N200 with a daughterboard for operating in 2.4GHz and 5GHz range. Besides, to improve the frequency accuracy, it had installed a GPS disciplined oscillator. A summary of the equipment characteristics is included in Table 4.1.

Conversion and Oscillator Performance	
ADC Sample Rate	100 MS/s
DAC Sample Rate	400 MS/s
Frequency Accuracy	2.5 ppm
Frequency Accuracy (with GPSDO)	0.01 ppm
Operative Frequency Range	2.4 - 2.5 GHz
	4.9 - 5.9 GHz

TABLE 4.1: USRP N200/XCVR2450 specifications

4.1.2 LabVIEW controller

The USRP transceiver is connected to the computer via Ethernet cable, getting an IP address through which the software will communicate and route the data flow. LabVIEW presents full compatibility with USRP platforms, integrating a specific package of functions and modules to control the hardware transceiver. Since this package includes multiple possibilities that exceed the necessities for this project, we will just review the process for establishing a connection between the computer and the USRP, focusing in the configuration parameters that significantly condition the proper link operation. In this line, Figure 4.1 represents the LabVIEW scheme for transmitting a stream of integers through the USRP transmitter.

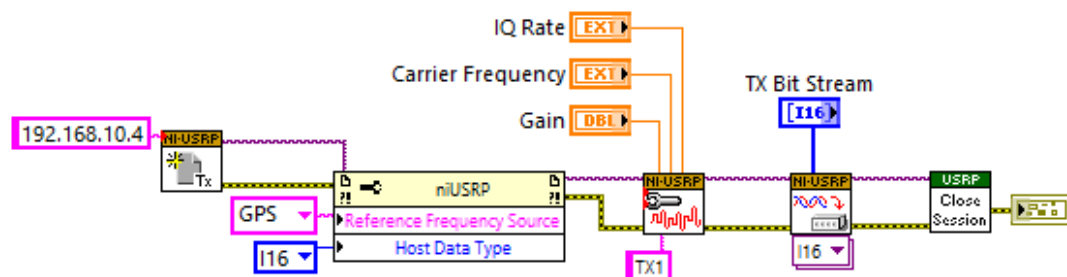


FIGURE 4.1: LabVIEW scheme for USRP transmission

The first step of the procedure is to open a session with the IP address of the USRP. Then USRP is configured through a setup block. At this point, the oscillator wanted to be used is specified. As it was previously stated, the hardware used for the experimental phase has a supplemental GPS disciplined oscillator that should be selected at this stage in order to improve the accuracy of the reference clock. Another parameter that can be selected is the input data type that will be provided to the USRP transmitter block. In this sense there are two data types that can be selected, complex double and 16-bit integer.

During the testbed process it was concluded that serving the data in integer representation had a better response from the transceiver. According to the USRP data interpretation of the 16-bit integer when transmitting a complex signal, the in-phase

and quadrature components have to be converted separately into the integer operating range and concatenate their values respectively.

The third block consists in establishing the parameters for the signal transmitted. At this stage, the carrier frequency, IQ rate and the analogue gain are established. Since the USRP has a certain range of operative frequencies and data rates, the values introduced can be coerced to the allowed parameters windows.

The following step is the transmission block, and given that the configuration was already determined, it only needs to collect the data stream and transmit it. Regarding this stage, another characteristic that was examined during the testbed implementation process is the influence of the amount of data served to the transmitter at a time. It was deduced that at high IQ rates, providing short data blocks to the transmitter may cause underflow issues. For this reason, is important to split the data transmitted in large blocks to avoid an eventual empty buffer. Finally, when all the data is transmitted the session is closed. In case some error appeared during the transmission it is reported to the user.

From the receiver perspective the communication between the computer and the USRP is similar. The configuration of the USRP is again carried out setting the data type and the reference clock. Equally, signal parameters like carrier frequency or data rate are established in the same way as in the transmitter. The only difference is the receiver block, that provides the data received by the USRP. If the 16-bit integer data type is selected, the user has to build the complex signal from the integer stream the receiver delivers.

4.2 Signal Adaptation

The implementation of a real RF communication link leads to deal with issues concerning the signal synchronisation and the inaccuracy between the clocks regulating the transmitter and receiver. As these problems were also present in our implementation, in this section we will explain their effect over the signal reception and how they were tackled.

4.2.1 Synchronization

In wireless communications, when the receiver sense the channel and acquire the data that is transmitted over the medium, it receives the signal asynchronously from the transmitter. This misalignment in the received signal makes impossible to identify the frame structure and therefore demodulate the data received. In order to solve this problem, the signal sent by the transmitter needs to include a predefined sequence so the receiver can localize it and synchronize the signal with the one that was transmitted.

It can be distinguished two different types of synchronizations, at frame level and at superframe level. The first one is used to identify the beginning of each frame so the symbols inside are aligned. The second type of synchronization is present in systems designed with a higher structure level and aims at identifying the position of the frame inside the superframe.

For the sake of a simple design, it was decided to build a structure of one frame that is repeated and continuously transmitted. With this assumption the only synchronization that was needed is at frame level. In order to accomplish this alignment, we will use the pilots sequence at the beginning of each frame as a synchronization reference. Since the pilots OFDM symbol is a deterministic sequence known at the receiver, it can be correlated with the signal received in order to get their positions. Besides, the pilots were generated using a Zadoff-Chu sequence, which has among other characteristic a high defined autocorrelation that ease the localization in a frame.

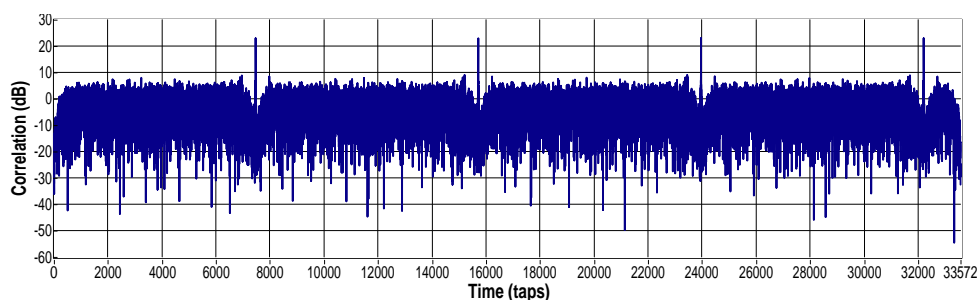


FIGURE 4.2: LabVIEW scheme for USRP transmission

Figure 4.2 shows the correlation between the signal received and the pilots sequence at the receiver end. In order to have a clear representation for this case the data window

processed has a length of 4 frames. As it is visible in the figure, the correspondent 4 peaks are clearly differentiate in the correlation identifying the position of the pilot sequence in each frame. When the receiver computes the correlation, it searches for the first complete pilot symbol and discards the data until that point. By this method, the system gets rid of the portion of frame that is incomplete in the window.

4.2.2 Phase error reduction

The main problem that showed up during the experimental stage was the appearance of phase error in the signal received. This problem was already affecting in the early tests with the OFDM scheme, presenting a received constellation with a circular shape. There were considered some possibilities that could cause this phase drift, like a wrong synchronization that was finally discarded after verifying a proper frame alignment. Nevertheless, it was shown that when activating the GPS disciplined oscillator of the USRP this effect was reduced, presenting a constellation at the receiver with just a slight twisting effect. The constellations received for the case in which the GPSDO is disabled and enabled are depicted in Figure 4.3a and Figure 4.3b respectively.

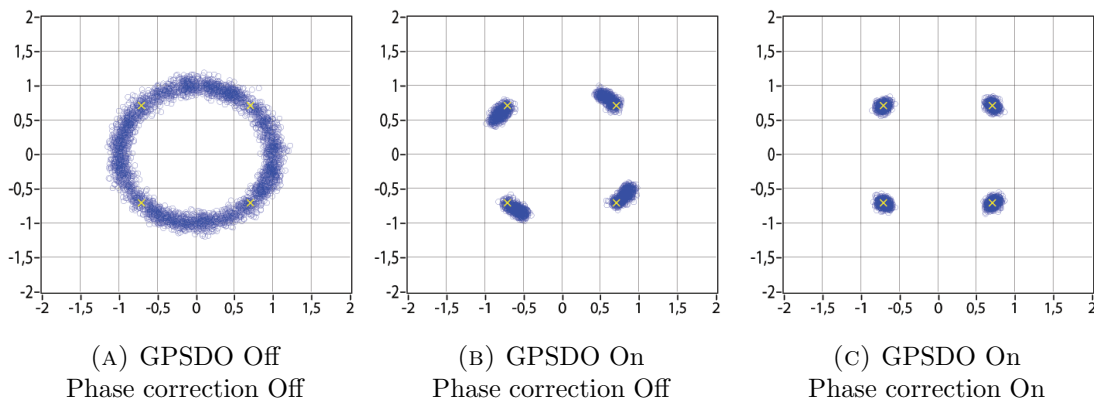


FIGURE 4.3: QPSK constellation received.

Based on the fact that this phase shift effect can be considered constant along the same OFDM symbol, it was decided to implement a method consisting in hard-coding the first data subcarrier of every OFDM symbol before the subcarrier allocation. By this procedure, the receiver knows the symbol mapped over this subcarrier and can evaluate the phase shift and apply this correction factor to the rest of subcarriers. The result of this phase correction aims at a good performance when the SNR level is high, as it is shown in Figure 4.3c. Nonetheless, for high SNR its correction capability will be limited

since the phase evaluated is highly deteriorated by the noise and applying it to the rest of subcarriers could have a spreading effect. Despite this last consideration, it can be estimated that the overall performance of this phase correction method overcome the inherent drawback of carrying out the experiments with the constant effect of a phase shift.

4.3 Real Link Scenario

In this section we will describe the conditions over which the testbed experiments were performed. In first place we will present the topology of the indoor environment where the experiment took place. After that, the scenario setup will be explained, including the configuration used for the transceivers.

Environmental description

For the experimental phase it was decided to carry out the measurements in an indoor scenario. In particular, the location chosen was the laboratory of the department. This scenario is characterized by a heterogeneous distribution of office furniture and laboratory equipment. The laboratory is divided in two parts by a high wardrobe providing a certain isolator effect on the activity taking place in the other section of the room. This fact was taken into account, making sure that any person working on the other section was not affecting the signal received. Nonetheless, the majority of the measurements were taken with the room empty or only with persons in the less disturbing zone of the laboratory. Figure 4.4 shows the scenario chosen for the experimental phase.

Scenario setup

The goal of the experiment was the acquisition of BER and BLER statistics for different values of SNR for the three waveforms studied. In order to get diverse values of SNR, it was decided to play with the distance between the transmitter and the receiver as well as with some obstacles to disturb the channel. For this purpose, the transmitter and

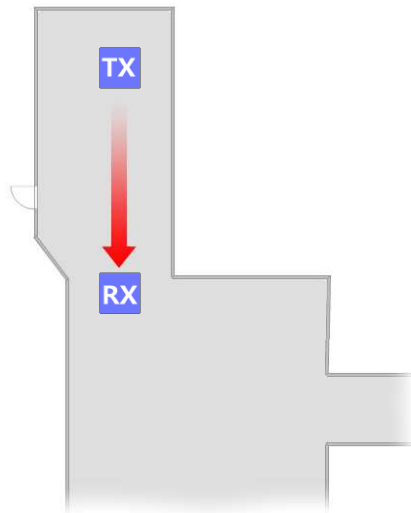
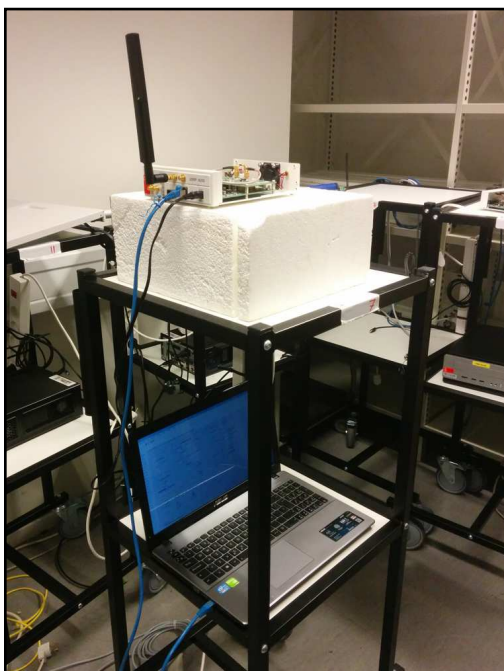


FIGURE 4.4: Map of the section used for the measurements

receiver were placed in trolleys to facilitate their mobility around the laboratory. This structure can be observed in Figure 4.5a and Figure 4.5a, representing the transmitter and receiver configuration respectively.



(A) Transmitter trolley



(B) Receiver trolley

FIGURE 4.5: Transmitter and receiver disposition

As it is shown in the receiver figure, a spectrum analyser was placed in the receiver

trolley to eventually contrast the signal to noise ratio estimated from the receiver USRP with the one measure in the spectrum analyser. Nevertheless, all the data was collected with the spectrum analyser turned off to avoid any possible interference with the USRP receiver.

The transmitter was settled to the upper corner of the room while the receiver was moving away for decreasing the power of the signal received. Along this process it was concluded that although the channel was relatively invariant in time, a slight modification of the receiver position can provoke an important variance in the level of the signal received. This can be justified by the multipath characteristic of an indoor environment and the shadowing effect of the obstacles present in the scenario.

USRP and link configuration

As it was explained in section 4.1.1 the hardware used for the experimental phase provides some flexibility when choosing parameters such as carrier frequency, IQ rate or gain. Since the array of data fed to the USRP is built with the outcome of the IFFT, the IQ rate will determine the sampling period and therefore the subcarrier spacing (Δf_{sc}) in the following relation:

$$IQ_{RATE} = \frac{1}{dt} = \Delta f_{sc} \cdot N_{IFFT} \quad (4.1)$$

In order to minimize the detrimental effect of the phase noise it was chosen a configuration with a high IQ rate of 12.5 MBauds to provide a wider spacing between subcarrier. Besides, as it was supposed, the phase noise was probed to diminish when selecting a lower carrier frequency, what led us to discard the 5GHz range and choose a frequency in the USRP low operation range. In this line and to avoid interference from Wi-Fi signals from the laboratory, it was chosen to operate at the japanese exclusive Wi-Fi channel, setting the carrier frequency to 2.484GHz. Table 4.2 summarize the USRP configuration selected for the experimental phase.

USRP and Link configuration	
Carrier frequency	2.484 GHz
IQ Rate	12.5 MBd (symbols/s)
Transmitter Gain	20 dB
Receiver Gain	20 dB
FFT Size	512
No. Subcarriers	300
Effective subcarrier spacing	24.4 KHz
Coding technique	Convolutional (rate 1/2)

TABLE 4.2: USRP and link configuration

4.4 Results

Before presenting the results obtained, we consider convenient to state a few facts and difficulties experienced in the preliminary tests as well as during the definitive measurement phase. First of all, it was shown since the beginning that there was a remarkable difference in the demodulation process delay when the encoder was enabled in comparison with the case it was switched off. Although this fact was also shown in the simulation phase, the difference in the experimental stage was even bigger. In light of this, we decided to keep a compromise between the processing time and the accuracy of the measurement gathered, establishing a minimum amount of packets processed per point of 5000.

Secondly, given the phase noise issues present from the beginning, a constellation graph was included in the receiver control panel allowing to monitor the QAM symbols just before the demodulation block. Thanks to this monitor we could verify a unstable behaviour in the constellation phase specially in the case of the Zero Tail technique. Finally, another consideration regarding the experimental phase is that it was decided to only consider two types of modulation, 4QAM and 16QAM.

BER

We will start by analysing the BER response of the three techniques for the 4QAM case. The results, shown in Figure 4.6, present a relatively close performance of OFDM and SC-FDM with a bit better response for the single carrier waveform specially when the encoder is enabled. On the other hand, the BER for Zero-Tail is higher for every SNR plotted. In this line is also noteworthy the parallelism between the coded and uncoded

performance. Moreover, it can be observed in the OFDM and SC-FDM responses the cross-point between the curves for the coded and not coded cases, situation also shown in the simulated results.

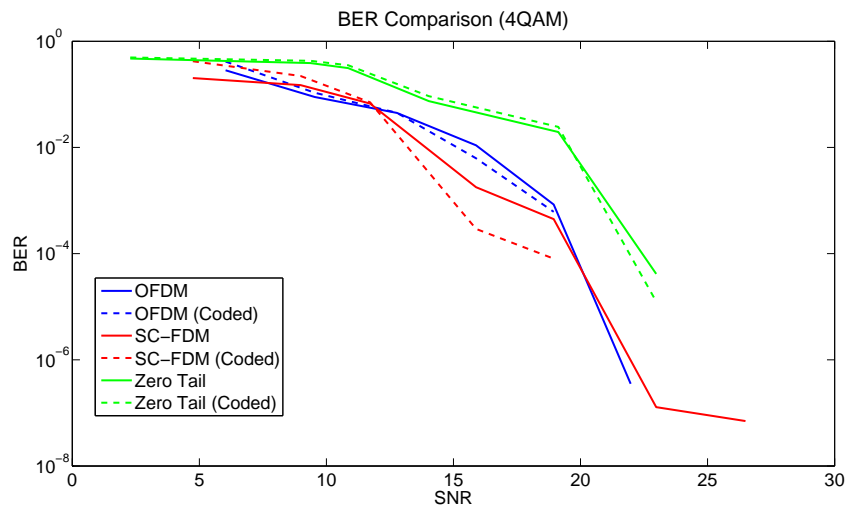


FIGURE 4.6: BER comparison for 4QAM

After analysing the results for 4QAM, the next step is to compare the BER of the three chosen waveforms under a more crowded constellation like 16QAM. The results for this modulation are shown in Figure 4.7. For the non-coded case, we can see a similar response for SNR values below 20dB, and from that level on the SC-FDM response gets a deteriorated appearing a gap of around 3dB in benefit of OFDM. Their respective coded curves show also a very close behaviour, presenting SC-FDM bit errors until 27 dB while the coding for OFDM corrects all the bit errors for SNR points evaluated above 22dB. Following the same tendency as in the 4QAM case, Zero-Tail present the worst performance for both coded and non coded curves. Besides, it also confirm the inability of the coding to improve the BER.

BLER

Continuing with the analysis of the three waveforms in this section we will focus on the BLER. In the same way as it was done for the BER we will compare the BLER performance for both coded and non-coded cases. The results for a 4QAM modulation

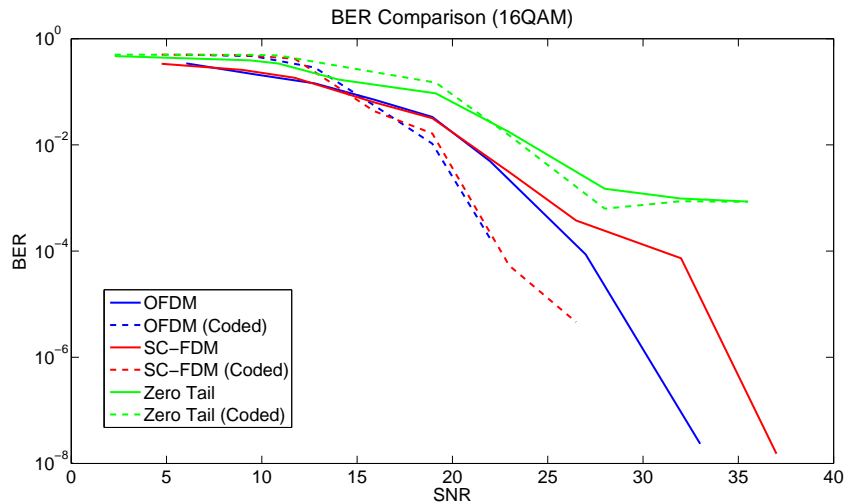


FIGURE 4.7: BER comparison for 16QAM

is depicted in Figure 4.8. On it we can observe that the appearance of some error-free frames does not start until the SNR reaches 10dB for the coded curves and 15dB for the non coded cases. Particularly, for the non coded curves the performance of the three techniques are quite similar with a slight worse behaviour for Zero-Tail. On the other hand, the BLER for the coded cases shows an improvement for OFDM and SC-FDM while coding for Zero-Tail doesn't provide the same enhancement.

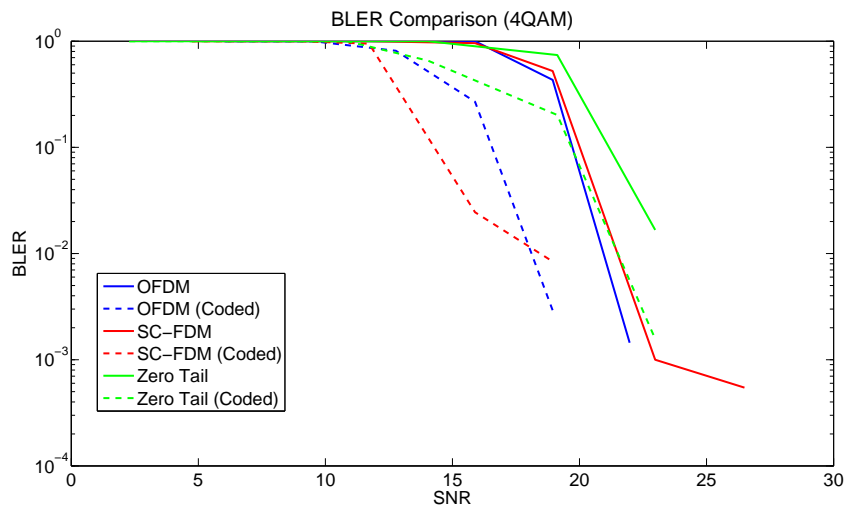


FIGURE 4.8: BLER comparison for 4QAM

The results gathered when the modulation selected was 16QAM are shown in Figure 4.9. On the plot it can be noticed a degradation of the SC-FDM performance for

the non coded case in relation with the 4QAM modulation, even reaching the Zero-Tail curve for certain values. Conversely, when the bit stream was encoded SC-FDM and OFDM have a relatively similar response.

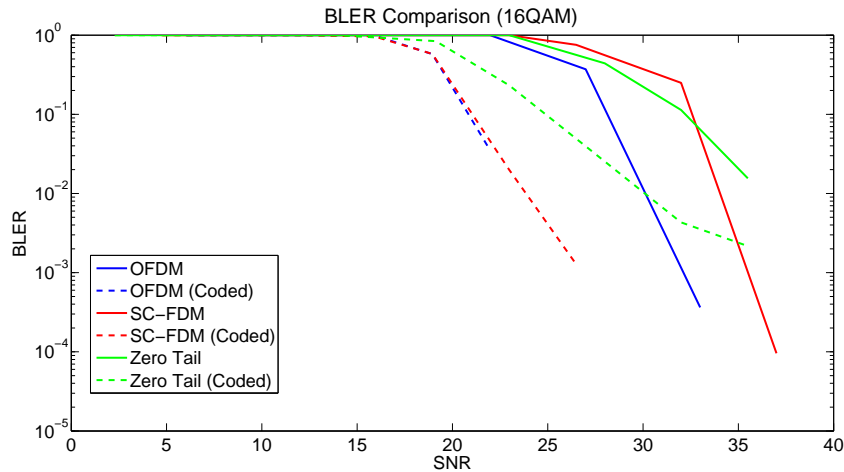


FIGURE 4.9: BLER comparison for 16QAM

Spectral Containment

In order to complete the evaluation of the different techniques, we finish with an analysis of the spectral containment for every candidate. As it is shown in Figure 4.10, the spectral representation of SC-FDM and OFDM have a very very close response. On the other hand, it can be seen that Zero-Tail has a much better power isolation in the frequency domain, creating a gap of about 10 dB with the other candidates. This low OOB emissions are justified in the smooth transition between symbols in time due to the low power tail and header as it is shown in Figure 4.11.

Summarizing, it can be concluded that the results throw a disappointing behaviour for Zero-Tail waveform in comparison with the other two candidates in terms of BER and BLER. As it was introduced at the beginning of the section, this may be caused by the result of the phase instability observed in the received QAM symbols. There are a couple of reasons that could justify this phase drift. In first place it could be caused by the way the phase is corrected, showing a sensibility to a hard-coded subcarrier at the beginning of the data band. The second reason is related with the way the pilots are created. Since the pilot sequence is processed as a data symbol, the insertion of the tail and header

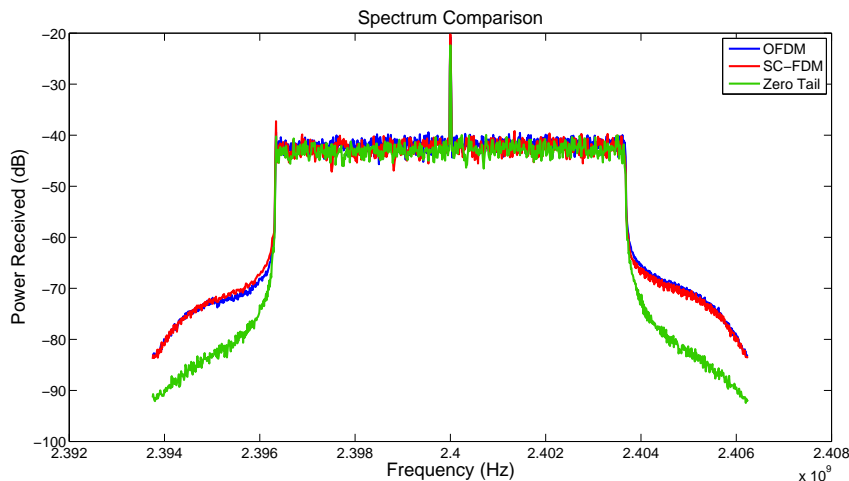


FIGURE 4.10: Spectrum comparison between the three techniques

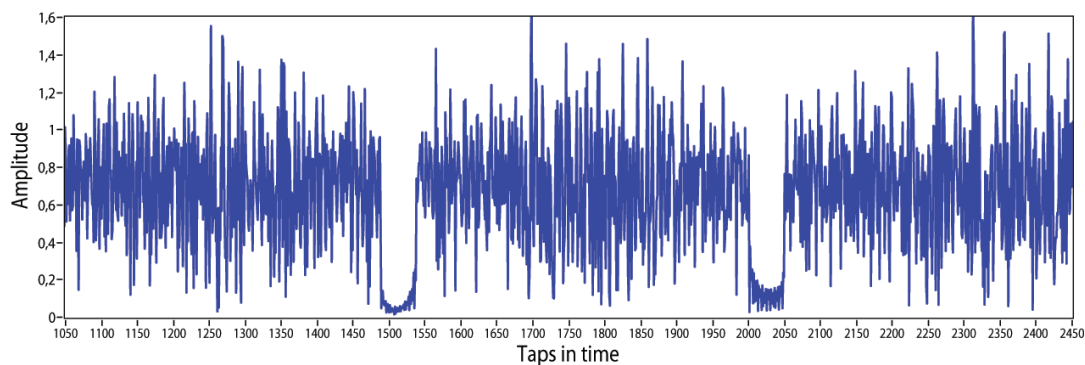


FIGURE 4.11: Time representation of Zero-Tail signal

previous to the FFT provokes a slightly rippled response in frequency that may affect to the equalization accuracy. Nonetheless, an optimization of the reference sequence for the pilots may overcome the performance gap. Finally, regarding the spectral containment, the OOB emissions for Zero-Tail are proved to have a better performance as it was presumed in the light of the theoretical analysis.

4.5 Summary

At the beginning of this chapter it was described the scenario, configuration and hardware used in the real link implementation carried out. The transceivers employed were introduced, resuming their main characteristics and operating features. The experiment scenario was presented, explaining also the methods concerning the synchronization and link adaptation. Moreover, a detailed exposition of the parameters used

for the experiment (e.g. carrier frequency, IQ rate...) was included to provide the link configuration over which took place the measurements. In the last part of the chapter the results gathered were presented and analysed, exposing the ideas and conclusions extracted from the figures.

Chapter 5

Conclusions

In this chapter it will be presented a brief summary of the project carried out to have an idea of the project phases and progression. Lately, it will continue with the exposition of the general conclusions obtained regarding the project process, goals and results. The chapter will finish by tracing what we consider would be the suitable lines of study in future works and how the evaluation methods designed in this project can be optimized.

5.1 Project Summary

The motivation of the project arise from the research stage of the 5th generation of wireless communications and specially in light of the uncertainty regarding most of its aspects that are still to be decided. Among the branches involved in the definition of the standards for this upcoming generation, one of the lines of research is related to the radio waveform that will be implemented. In this line, several are the options nowadays considered to be suitable candidates for this objective. These waveforms under study can be divided in two main groups, the ones that are based on traditional OFDM, and the ones that in some way tackle the problem from another perspective. In our department we consider promising a new idea based on the DFT-s-OFDM but aiming to cope with the inefficiency of a hard-coded CP length, separating the radio numerology from the channel characteristics.

This project is framed in the study of the performance of this technique in comparison with the technologies already implemented for 4G in order to evaluate the potential advantages of this Zero-Tail DFT-s-OFDM waveform. To carry out this task we divided the project in two main stages. In the first stage the different schemes were implemented in the LabVIEW software platform studying their performance over a simulated link. The second phase consists in the implementation of a real link using USRP transceivers to evaluate the different techniques and give a solid idea on the real performance of this radio waveforms.

5.2 Conclusions

From the simulation phase results we can conclude that Zero-Tail has a similar response to SC-FDM in terms of BER and BLER with a slight degradation in terms of PAPR depending on the chosen size for the low power tail of the signal. Nonetheless, the PAPR performance for Zero Tail is still widely better than OFDM, what improves the response of the power amplifiers. Besides, it was studied the OOB emissions, revealing that Zero-Tail waveforms have a more contained spectral response, providing the possibility of a more efficient usage of the spectrum.

Regarding the outcome of the experimental phase, it should be stated that the results for Zero-Tail are quite unexpected, differing from the simulation conclusions for the BER and BLER. Nonetheless, we consider two possible facts that could strongly affect the response for Zero-Tail in comparison with OFDM and SC-FDM. The first one is related with the way the pilots are generated. The insertion of a header and tail of zeros prior to the DFT block, cause a certain ripple in the frequency amplitude that contaminates the flat characteristic of the Cazac sequence used for the pilots. The second fact that could have caused the poor performance of Zero-Tail is the way the phase noise was corrected, adding a hard-coded subcarrier at the end of the useful spectrum. This reference subcarrier is placed in the most unstable part of the curly response of Zero-Tail, what may wrongly estimate the phase shift for the rest of the symbol turning the phase correction into a phase error source.

From a general perspective it may be stated that the project progression was affected by the time consuming acquaintance with the hardware used for the real link

implementation and the lack of experience in the LabVIEW programming. Nonetheless, these two facts meant a constructive and interesting experience for the author giving an important background on the tools used.

5.3 Future lines of study

A global overview on the project carried out and the results obtained suggest several branches that are interesting to investigate. Most of them arise from the fact that the unexpected performance limitations of Zero-Tail couldn't be thoroughly addressed by the lack of time. Those lines of study are:

- Analyse the Zero-Tail discrepancy between the simulated and real link results. We suggest the consideration of the two suspicious causes presented in the conclusions sections by verifying or discarding their effect over the BER and BLER performance.
- For instance, in case the ripple behaviour of the Zero-Tail pilots is revealed to play a strong role in the performance degradation due to the equalization, it could be interesting the study of the pilots generation through other sequence pattern.
- Optimization of the data collection process, specially for the case in which the coding is enabled. Decreasing the process delay will lead to a more efficient measurement phase, being able to gather a huge amount of data in a short time.

Bibliography

- [1] Nadjia Kara, Omneya Issa, and Alain Byette. Real 3g wcdma networks performance analysis. In *Local Computer Networks, 2005. 30th Anniversary. The IEEE Conference on*, pages 7–pp. IEEE, 2005.
- [2] Johan Bergman, Dirk Gerstenberger, Fredrik Gunnarsson, and Stefan Ström. Continued hspa evolution of mobile broadband. *Ericsson Review*, 1:7–11, 2009.
- [3] Sadayuki Abeta. Toward lte commercial launch and future plan for lte enhancements (lte-advanced). In *Communication Systems (ICCS), 2010 IEEE International Conference on*, pages 146–150. IEEE, 2010.
- [4] Cisco. Cisco visual networking index: Global mobile data traffic forecast update 2014–2019 white paper. February, 2015.
- [5] Preben Mogensen, Kari Pajukoski, Esa Tirola, Eeva Lähetkangas, Jaakko Vihriälä, Seppo Vesterinen, Matti Laitila, Gilberto Berardinelli, Gustavo Wagner Oliveira Da Costa, Luis Guilherme Uzeda Garcia, et al. 5g small cell optimized radio design. In *IEEE*, 2013.
- [6] Gilberto Berardinelli, Kari Pajukoski, Eeva Lähetkangas, Risto Wichman, Olav Tirkkonen, and Preben Mogensen. On the potential of ofdm enhancements as 5g waveforms. In *Vehicular Technology Conference*, 2014.
- [7] Moray Rumney. 3gpp lte: Introducing single-carrier fdma. *Agilent Technologies White Paper*, 2008.
- [8] Hyung G Myung, Junsung Lim, and David Goodman. Single carrier fdma for uplink wireless transmission. *Vehicular Technology Magazine, IEEE*, 1(3):30–38, 2006.

-
- [9] Gilberto Berardinelli, Fernando ML Tavares, Troels B Sorensen, Preben Mogensen, and Kari Pajukoski. Zero-tail dft-spread-ofdm signals. In *Globecom Workshops (GC Wkshps), 2013 IEEE*, pages 229–234. IEEE, 2013.
- [10] Marko Lampinen, Felipe Del Carpio, Tero Kuosmanen, Tommi Koivisto, and Mihai Enescu. System-level modeling and evaluation of interference suppression receivers in lte system. In *Vehicular Technology Conference (VTC Spring), 2012 IEEE 75th*, pages 1–5. IEEE, 2012.
- [11] Simon Haykin, Mathini Sellathurai, Yvo de Jong, and Tricia Willink. Turbo-mimo for wireless communications. *Communications Magazine, IEEE*, 42(10):48–53, 2004.
- [12] Telesystem Innovations. Lte in a nutshell. *White Paper*, 2010.
- [13] Omar Arafat, K Dimyati, Fatima Seeme, Arman Md Mushtaq, and HM Farhad. A comparative simulation of mobile wimax physical layer performance for zero-force (zf) and minimum mean square error (mmse) channel equalizers. *International Journal of the Physical Sciences*, 5(16):2503–2515, 2010.